Revista Mexicana de Ciencias Geológicas, v. 25, núm. 2, 2008, p. 314-333

U-Pb and $^{40}Ar/^{39}Ar$ geochronology of the coastal Sonora batholith: New insights on Laramide continental arc magmatism

Ernesto Ramos-Velázquez[1,2,*], Thierry Calmus[1], Victor Valencia[3], Alexander Iriondo[4,5], Martín Valencia-Moreno[1], and Hervé Bellon[6]

[1] Estación Regional del Noroeste, Instituto de Geología, Universidad Nacional Autónoma de México, Apartado Postal 1039, Hermosillo, Sonora, 83000, México.
[2] Universidad Autónoma de Baja California Sur, Departamento de Geología, Apartado Postal 19-B, La Paz, B.C.S., 23080, México.
[3] University of Arizona, Department of Geosciences, Tucson, Arizona 85721, USA.
[4] Centro de Geociencias, Universidad Nacional Autónoma de México (UNAM), Campus Juriquilla 76230, Juriquilla, Querétaro, México.
[5] Department of Geological Sciences, University of Colorado at Boulder, Boulder, Colorado 80309, USA.
[6] UMR 6538, Domaines Océaniques, IUEM, Université de Bretagne Occidentale, 6, Av. Le Gorgeu, BP 809, F-29285, Brest Cedex, France.
** eramos@uabcs.mx*

ABSTRACT

The coastal Sonora batholith comprises a series of Cretaceous granitoids that intruded a metasedimentary basement of possible Mesozoic age. They are partially covered by Tertiary volcanic flows and pyroclastic rocks. In order to elucidate the crystallization and cooling history of the granitoids, nine rock samples were collected from Bahía Kino to Punta Tepopa. Eight samples dated by U-Pb zircon geochronology show that the Coastal Sonora batholith was emplaced during the Late Cretaceous, between 90.1 ± 1.1 and 69.4 ± 1.2 Ma. The interval of ~20 Ma between the different stages of crystallization indicate that magmatism was relatively static within coastal Sonora, although the magmatic arc recorded an eastward migration as a whole during Cretaceous and Paleogene. In addition, three of these samples were also dated by $^{40}Ar/^{39}Ar$ in biotite and K-feldspar separates. Ages vary from ~74 to 67 Ma in biotite and from ~68 to 42 Ma in K-feldspar. We interpret these ages as the cooling progression of the batholith, associated with exhumation of the region before the Basin and Range extension. Furthermore, these results show a local trend towards younger ages to the north of the batholith, and they are in good agreement with the model of a general eastward migration of the Cretaceous-Tertiary magmatic arc in northwestern Mexico. In general, the available ages suggest that the arc moved slowly across Baja California between 140 and 105 Ma, and continued its eastward migration across the eastern portion of Baja California and Sonora between 105 and ~60 Ma. According to the isotopic ages, the Coastal Sonora batholith would be the westernmost part of the Laramide magmatic event (~90 – 40 Ma). Thus, on the basis of new and available geochronologic, petrographic, and geochemical data, we propose that the Coastal Sonora batholith and the eastern portion of the Peninsular Ranges batholith belong to a single magmatic arc, which was separated during the continental breakup and rifting of the Gulf of California in the Tertiary.

Keywords: geochronology, U-Pb, $^{40}Ar/^{39}Ar$, Cretaceous-Tertiary magmatic arc, Laramide, Coastal Sonora batholith, Mexico.

RESUMEN

El batolito Costero de Sonora comprende una serie de granitoides cretácicos que intrusionan un basamento metasedimentario de posible edad Mesozoica. Están cubiertos parcialmente por rocas piroclásticas y flujos volcánicos terciarios. Para conocer la historia de cristalización y enfriamiento de los granitoides se colectaron nueve muestras de granitoides desde Bahía Kino hasta Punta Tepopa. Ocho de ellas fueron fechadas usando geocronología U-Pb en circones y muestran que el batolito Costero de Sonora fue emplazado durante en Cretácico Tardío, entre 90.1 ± 1.1 y 69.4 ± 1.2 Ma. Este rango de edades de cristalización (~20 Ma) sugiere que el magmatismo fue relativamente inmóvil en la región costera actual de Sonora, aunque el arco magmático registró en conjunto una migración hacia el este durante el Cretácico y Paleógeno. Además, tres de estas muestras fueron también fechadas por $^{40}Ar/^{39}Ar$ en separados de biotita y feldespato potásico para evaluar el enfriamiento de los cuerpos graníticos. Las edades $^{40}Ar/^{39}Ar$ varían de ~74 a 67 Ma en biotita, y de ~68 a 42 Ma en feldespato potásico. Interpretamos estas edades como el resultado del enfriamiento del batolito, asociado con una importante exhumación de la región costera de Sonora. A nivel del batolito Costero de Sonora, las intrusiones muestran edades más jóvenes en la parte norte del batolito, sin contradecir el modelo general de una migración hacia el este del arco magmático Cretácico-Terciario en el noroeste de México. En general, las edades disponibles sugieren que el arco migró lentamente a través de Baja California entre 140 y 105 Ma, y continuó a través de la porción oriental de Baja California y Sonora entre ~105 y 60 Ma. De acuerdo con las edades isotópicas obtenidas en la región costera de Sonora, el batolito Costero de Sonora puede representar la parte más occidental del evento magmático Larámide (~90 – 40 Ma). Así, con base en los nuevos datos obtenidos y en los datos geocronológicos, petrográficos y geoquímicos disponibles, proponemos que el batolito Costero de Sonora y la porción este del batolito de las Sierras Peninsulares pertenecen a un mismo arco magmático, el cual fue separado durante la ruptura continental y el rifting del Golfo de California en el Terciario.

Palabras clave: geocronología, U-Pb, $^{40}Ar/^{39}Ar$, arco magmático Cretácico-Terciario, Laramide, batolito Costero de Sonora, México.

INTRODUCTION

The geologic evolution of northwestern Mexico since the Jurassic has been associated with the interaction between the North American and oceanic plates of the Pacific realm (Dickinson and Lawton, 2001). One of the main consequences of this interaction has been the magmatism along the continental margin that originated a series of batholiths, currently exposed in southwestern USA (California and Arizona) and northwestern Mexico (Baja California peninsula and in the states of Sonora and Sinaloa). As a whole, these batholiths are oriented NW-SE, subparallel to the paleotrench. In detail, Cretaceous plutons in Sonora display a widespread geographic distribution, due to the great extent of magmatism during Laramide time and to the disruption related to the Basin and Range extension. Nevertheless, it is possible to recognize a NNW-SSE distribution with distinctive petrographic and geochemical characteristics, as well as cooling ages.

In California and Baja California peninsula, the Peninsular Ranges batholith (PRB) is composed by two magmatic belts, known as the western Peninsular Ranges batholih (WPRB) and the eastern Peninsular Ranges batholith (EPRB). Both belts are subparallel to the long axis of the peninsula (NW-SE), and such division is based on geochemical, petrographic, geophysical and geochronological data (Gastil, 1975; Langenheim and Jachens, 2003). The WPRB was probably developed on oceanic lithosphere, and is composed mainly of gabbroic to monzogranitic plutonic rocks, with U-Pb zircon ages ranging between 140 and 105 Ma (Silver *et al*., 1979; Silver and Chapell, 1988). The EPRB was developed on continental lithosphere, and is dominated by tonalite, trondjhemite, and K-poor granodiorite, with U-Pb zircon ages from 105 to 90 Ma (Silver *et al*., 1979; Silver and Chapell, 1988; Walawender *et al*., 1990). The potassium enrichment in the EPRB rocks, as well as the Ti enrichment, higher $^{87/86}Sr$ and higher εNd towards the east (Ortega-Rivera, 2003) suggest an interaction of magmas with preexisting crust.

The lithospheric differences of the substratum in which the granitoids from the WPRB and the EPRB were emplaced have been used to propose several tectonic models for the region. These models have been summarized by Wetmore *et al*. (2002) and are: 1) a single eastward migrating arc developed across a pre-Triassic suture between oceanic and continental lithospheres (Walawender *et al*., 1991; Thomson and Girty, 1994); 2) an exotic island arc accreted to the North American margin across a non-terminal suture (Johnson *et al*., 1999; Dickinson and Lawton, 2001); 3) the reaccretion of a rifted and fringing arc to the North American margin (Gastil *et al*., 1981; Busby *et al*., 1998). Wetmore (2003) showed that these models are inconsistent with the geologic evidence, because they do not consider the variations of the WPRB to the north and south of the Agua Blanca fault. Wetmore *et al*. (2002) proposed that the WPRB evolved during the Early Cretaceous within two

different tectonic blocks: a continental magmatic arc to the north (Santiago Peak arc segment), and an island arc to the south (Alisitos arc segment). Later, these two arc segments were joined due to the accretion of the island arc at the end of the Early Cretaceous.

Within continental Mexico, mainly in Sonora and Sinaloa, numerous batholiths were formed between 90 and 40 Ma during the Laramide orogeny. These batholiths form a NW-SE belt, which is known as the Laramide plutonic belt (Valencia-Moreno *et al*., 1999). This belt consists mainly of granodioritic to tonalitic plutons and subordinated bodies of diorite and granite, with U-Pb zircon ages of 90 to 40 Ma, younging eastward (Damon *et al*., 1983b; Roldán-Quintana, 1991; Valencia-Moreno *et al*., 1999; Valencia-Moreno *et al*., 2001; Henry *et al*., 2003; Valencia-Moreno *et al.*, 2006). The coastal Sonora batholith (CSB) and batholiths further east in Sonora and Sinaloa are interpreted to be a continuation of the EPRB, which is presently separated from Baja California by the Gulf of California. The EPRB and the CSB are related to the subduction of the Farallon plate beneath North America during the Late Cretaceous and early Tertiary. The eastward migration of the magmatic arc has been interpreted as a result of the increase in the convergence rate between both plates and of the gradual flattening of the slab (*i.e.*, Coney and Reynolds, 1977; Gastil, 1983; Dickinson, 1989). In Sonora, Sinaloa, Durango and Chihuahua, the Laramide plutons form a well defined belt, with an overall NW-SE orientation (Barton *et al*., 1995; Valencia-Moreno *et al*., 2001; Henry *et al*., 2003), subparallel to the Pacific margin (Figure 1), which suggests that: 1) Laramide magmatism was associated to the subduction of Farallon plate, and 2) the trench geometry has been steady since Late Cretaceous.

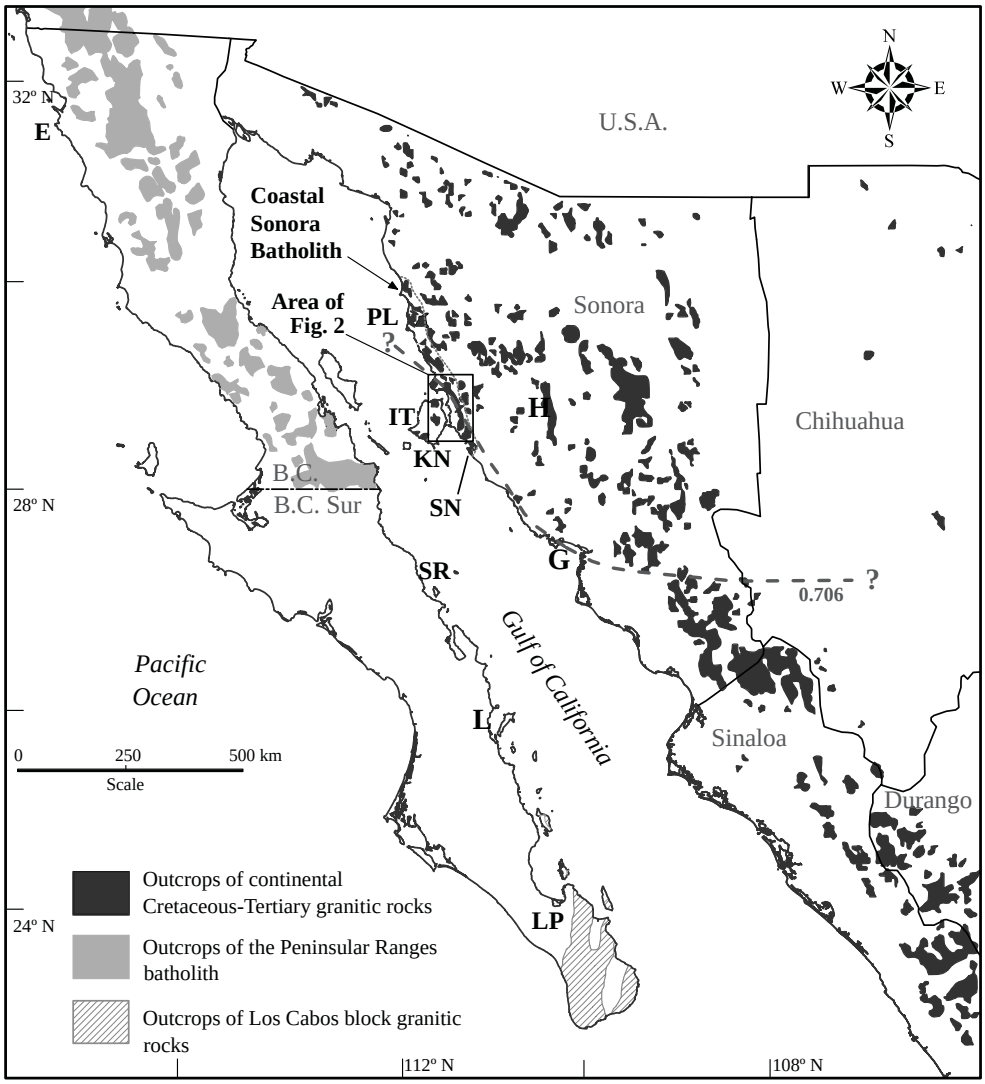

Figure 1. Regional distribution of early Cretaceous-late Tertiary igneous outcrops, in NW Mexico, and location of the Coastal Sonora batholith. The hypothetical location of the Proterozoic North America, based on the initial values of $^{87}Sr/^{86}Sr$ of 0.706, from Valencia-Moreno *et al*. (2001) is included. Localities mentioned in the text: B.C.: Baja California, E: Ensenada, G: Guaymas, H: Hermosillo, IT: Isla Tiburón, KN: Kino Nuevo, L: Loreto, LP: La Paz, PL: Puerto Libertad, SR: Santa Rosalía.

Previous studies of the Mexican Laramide batholiths have focused mainly on their geochemical characteristics (Roldán-Quintana, 1991; Valencia-Moreno *et al*., 1999, 2001, 2003; Vargas-Navarro, 2002), geochronology (Henry *et al*., 2003) and their relation to mineralization (Staude and Barton, 2001; Barton *et al*., 1995; Wodziki, 1995; Valencia-Moreno, 1998).

This study presents new geochronological data on three intrusive units from the CSB, between Bahía Kino and Punta Tepopa (Figure 1). Six samples were dated by U-Pb zircon analysis. Three of these samples were analyzed by $^{40}Ar/^{39}Ar$ geocronology on biotite and K-feldspar to constrain the thermal history from crystallization to cooling below the Ar-Ar closure temperature of K-feldspar. In addition a K-Ar analysis was conducted on one andesite whole rock sample.

PREVIOUS STUDIES

Several studies have been published on the magmatic and tectonic evolution of the coastal Sonora batholith (CSB) and its relationship with the geological framework of the North America Cordillera. Anderson and Silver (1969) reported in an abstract U-Pb isotopic ages from 100 ± 3 to 82 ± 3 Ma in zircons from several granitoids of the coast of Sonora. In coastal Sonora, metasedimentary basement rocks of possible Carboniferous or Jurassic age were intruded by Cretaceous to early Tertiary granitic rocks, and later covered by Tertiary volcanic rocks (Gastil and Krummenacher, 1977). These authors report nine biotite and hornblende K-Ar ages on plutonic rocks that range between 91.0 ± 1.8 to 59.9 ± 1.2 Ma, including an age of 85.1 ± 1.7 Ma for an andesitic dike. A K-Ar age of 83 ± 2 Ma was reported by Mora-Alvarez (1992) for a granodiorite of the Bahía Kino region.

The geochemical compositions of the CSB have been presented elsewhere (Valencia-Moreno *et al*., 2001, 2003; Vargas-Navarro, 2002). Vargas-Navarro (2002) summarizes petrographic and isotopic variations of batholiths on both sides of the Gulf of California. The major-element contents of the CSB rocks are similar to those of the EPRB, but show a tendency to be more alkaline. Variations in the $^{87}Sr/^{86}Sr$ and $^{143}Nd/^{144}Nd$ isotopic ratios were interpreted as reflecting compositional changes in the Proterozoic and Paleozoic basement (Valencia-Moreno *et al*., 2001). Towards the west, the CSB shows less crustal contamination ($^{87}Sr/^{86}Sr$ <0.706 and εNd >3.5) whereas, eastwards, the crustal contamination increases ($^{87}Sr/^{86}Sr$ >0.706 and εNd <3.5). The $^{87}Sr/^{86}Sr$ = 0.706 ratio isopleth may reflect the southwestern limit of the Precambrian basement of North America (Valencia-Moreno *et al*., 2001). The contour of the 0.706 initial $^{87}Sr/^{86}Sr$ line is not well constrained north of the CSB, but is better defined in northern Baja California, where it follows a NNW direction from San Felipe, Baja California (Gromet and Silver, 1987), to the northeasternmost part of the Peninsular Range batholith. There, the 0.706 initial $^{87}Sr/^{86}Sr$ line coincides mostly with the Agua Caliente fault in the Perris block, and with the San Jacinto fault zone, bording the San Jacinto Mountains to the west (Kistler *et al*., 2003).

Isotopic ages of the Laramide intrusives in northwestern Mexico are numerous, and document its magmatic evolution. Near the coast of the Gulf of California, intrusive rocks yielded U-Pb ages on zircons ranging between 100 and 82 Ma (Anderson and Silver, 1969), and the oldest K-Ar hornblende ages, from 90 to 60 Ma (Gastil and Krummenacher, 1977; Mora-Alvarez and McDowell, 2000; Henry *et al*., 2003). Eastward, the ages range from 63 to 49 Ma as indicated by K-Ar ages on hornblende and biotite in eastern Sonora (Damon *et al*., 1983a; Shafiqullah *et al*., 1983; McDowell and Roldán-Quintana, 1993; McDowell and Mauger, 1994). The U-Pb zircon ages of central Sonora intrusive rocks range from 63 to 56 Ma, being younger than these from the CSB (McDowell and Roldán-Quintana, 1993; McDowell and Mauger, 1994).

Numerous ages for volcanic rocks of the Cretaceous-Tertiary interval have been obtained by the K-Ar method, an to a lesser extent by $^{40}Ar/^{39}Ar$ and U-Pb; they also show younging ages from west to east, supporting the interpretation of an eastward migration of the magmatic arc (Damon *et al*., 1983a; McDowell and Mauger, 1994; Gans, 1997; McDowell *et al*., 2001; Henry *et al*., 2003; Valencia-Moreno *et al*., 2006).

GEOLOGICAL FRAMEWORK

Rocks of the Sonora coastal region and Isla Tiburón consist of Mesozoic(?) metasedimentary rocks intruded by granitoid rocks and an unconformable cover of mid-Tertiary volcanic rocks. The regional structural trend and the strike of metamorphic units have a general orientation subparallel to the coast, forming horsts separated by basins filled with Pliocene to Quaternary sediments.

In the Kino Nuevo-Punta Tepopa area (Figure 2), the oldest unit corresponds to roof pendants of greenschist facies metasandstone, marble and metaconglomerate. In the Cerro El Tordillo area (Figure 2), the thickness of this unit reaches 350 m. Metamorphic rocks display a strong metamorphic foliation parallel to bedding, but the strike of foliation is very heterogeneous. Locally, the metamorphic unit is affected by ductile shear zones, parallel to foliation. Close to the plutons of the CSB, metamorphic rocks exhibit contact metasomatism with formation of wollastonite and garnet in calcareous rocks, and hornblende, kyanite and muscovite in sandstone. Gastil and Krummenacher (1977) suggests a Mesozoic age for this metamorphic unit on the basis of lithological correlations with a similar unit located to the north of Desemboque, which contains *Trigonia inexpectata*, of probable Early Jurassic age.

The CSB can be divided in two belts: 1) an eastern NNW-SSE striking belt, from Punta San Nicolás to Puerto

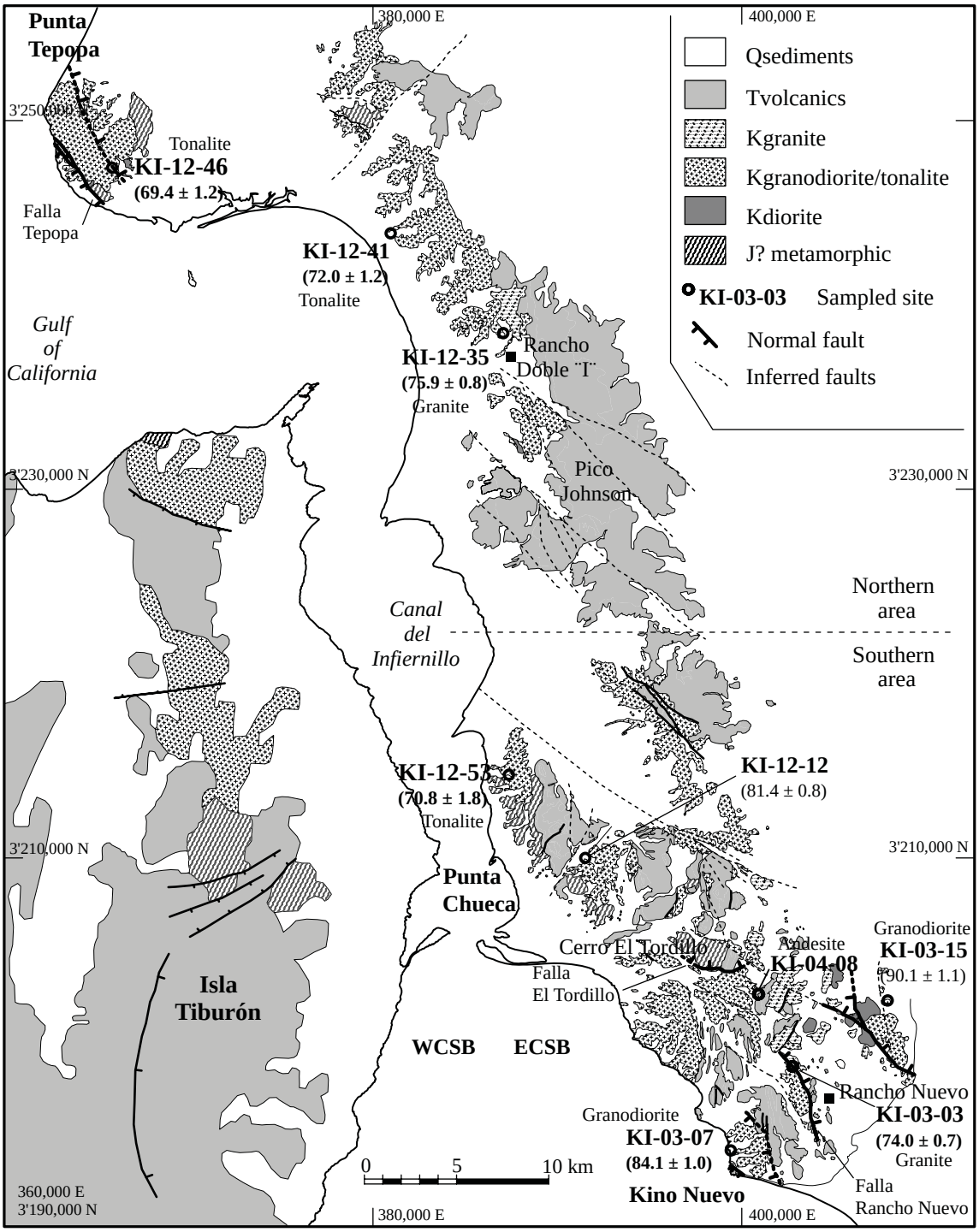

Figure 2. Geologic map of the study area, showing location of samples dated in this study, and the U-Pb zircon ages. Tertiary volcanic rocks are grouped in a single geologic unit. ECSB: Eastern Coastal Sonoran Batholith, WCSB: Western Coastal Sonoran Batholith.

Libertad (Figure 1), that is 160 km long and 10 km wide and corresponds to a westward tilted block, almost perpendicular to the main direction of Tertiary extension; 2) a 70-km-long western belt composed of several plutons that crop out in Isla Tiburón and Punta Tepopa (Figure 2). To the east, the CSB is limited by the ~100 km wide Hermosillo coastal alluvial plain, which separates the CSB from the plutonic rocks of the Hermosillo area.

The CSB consists mainly of granodioritic and tonalitic plutons, with subordinated bodies of diorite and granite, besides of granitic dikes with aplitic and pegmatitic textures, and andesitic hipabysal intrusions. The oldest intrusive

unit is the Puerto Rico diorite (Figure 2), which crops out in the CSB as small isolated bodies. In the northern part of the CSB, the Puerto Rico diorite is dark gray, fine- to coarse-grained and consists mainly of plagioclase, biotite, hornblende, scarce quartz, with apatite and zircon as accessory minerals. A magmatic foliated texture is defined by a preferential orientation of biotite, hornblende and plagioclase.

The Kino granodiorite and Tepopa tonalite (Figure 2) intrude the diorite; in Figure 2 they are not differentiated because contacts are transitional and irregular. The Kino granodiorite crops out mainly in the southern part of the area, between Kino Nuevo and Punta Chueca. It is light gray and coarse grained, composed of plagioclase, quartz, K-feldspar, biotite and hornblende. In some samples, the granodiorite presents a slight ductile deformation, underlined by irregular mineral contacts and undulating extinction of quartz crystals, as well as deformed biotite altered to chlorite, and hornblende altered to epidote and subrounded K-feldspar. The Tepopa tonalite crops out mainly in the northern part of the area, between Punta Tepopa and the NE of Pico Johnson (Figure 2). The tonalite is light gray to almost white in color, and is composed of plagioclase, quartz, biotite and hornblende, with zircon, sphene and apatite as accessory minerals. The texture is fine grained and equigranular, with a higher content of plagioclase and biotite than the Kino granodiorite. Intrusive contacts of the Kino granodiorite and Tepopa tonalite within the diorite are very straight and sharp, and crosscut by dikes. A 5–10 cm wide alteration zone is observed within the granodiorite, along the contact, characterized by a parallel recrystallization of quartz and biotite. All these data suggest that the plutons were emplaced at relatively cold conditions, with low thermal contrast between the host rock and intrusive, as is showed in several localities.

The Rancho Nuevo granite is the youngest unit of the CSB. It crops out extensively in the southeastern area of the CSB, and, towards the north, only around the Rancho Doble I locality (Figure 2). The Rancho Nuevo granite is reddish in color and coarse - to very coarse-grained, and its mineralogy of consists mainly of K-feldspar phenocrysts as long as 5 cm, quartz, plagioclase, biotite and hornblende, with apatite and zircon as accessory phase. K-feldspar is commonly altered to sericite along intracrystalline fractures. The characteristic reddish color is due to the oxidation of biotite. Intrusive contacts are sharp and characterized by textural changes and by the presence of local foliation. For instance, in the KI-12-35 locality, near Rancho Doble I (Figure 2), the contact between Rancho Nuevo granite and Kino granodiorite consists of two 50-cm-wide zones with distinct textures, developed in the granite. The closest zone to the granodiorite displays a strong foliation along the contact. The second one, with porphyritic texture, is characterized by phenocrysts of K-feldspar, plagioclase, biotite and quartz, in a fine-grained matrix of quartz and plagioclase. The texture and foliation changes are restricted to a very thin zone along the contact, suggesting a subsolidus flow (*i.e.*, Vernon, 2000) during the intrusion of the Rancho Nuevo granite into the Kino granodiorite. An aplitic and pegmatitic dike system, genetically related to the Rancho Nuevo granite, has a wide distribution in the area and cuts across all the granitic and metamorphic units. The width of dikes varies from 2–3 cm to about 1 m.

The Tordillo hypabisal andesite unit is spatially associated with the Kino granodiorite in the southern part of the area. The Tordillo andesite is gray and has a porphyritic texture characterized by phenocrysts of plagioclase in an aphanitic matrix, with sparce biotite crystals.

The CSB and metasedimentary are unconformably overlain by volcanic rocks that include rhyolite, andesite, tuff and basalt, associated with the activity of the Tertiary magmatic arc (Damon *et al*., 1983b), with a total composite thickness of around 400 m. The coastal zone of Sonora is partially covered by Pliocene-Quaternary sediments, which belong to deltaic deposits of the Río Sonora, dunes and marine terraces.

The CSB is affected by two sets of extensional faults. The less conspicuous set has a nearly E-W orientation, and includes the north dipping Tordillo normal fault (Figure 2). The more developed set is oriented NNW-SSE and controls the morphology of the coastal region; the west dipping Rancho Nuevo fault and the east dipping Tepopa fault belong to this last set. The Rancho Nuevo fault has a single normal slip, whereas the Tepopa fault presents two generations of superimposed kinematic indicators; the oldest one indicates a normal slip and the youngest one indicates a lateral slip, with a minor normal component (Figure 3). This structural information reflects the post-12 Ma opening of the

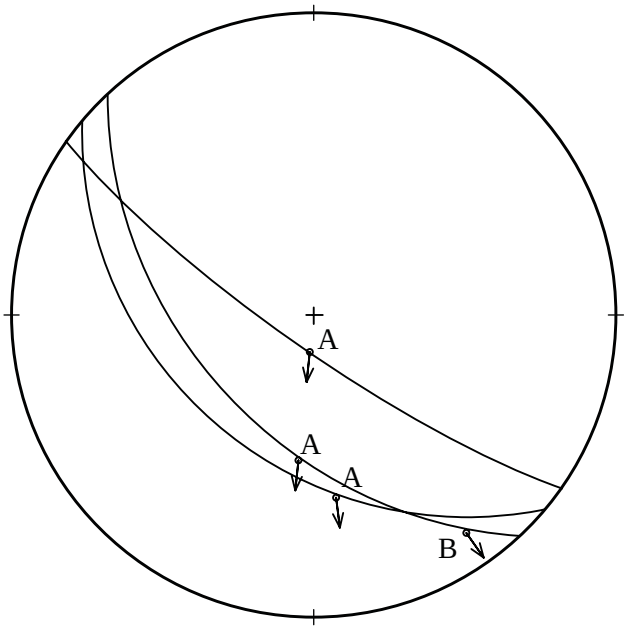

Figure 3. Structural data from a single plane in Tepopa fault, showing two stages of movement overprinted, normal (A) on normal plus lateral (B).

Gulf of California in this part of its eastern margin. After the subduction stopped at 12.5 Ma, continental breakup occurred along a SW-NE to W-E strike of extension, and was followed, since 6 Ma, by a right-lateral motion along NW-SE to NNW-SSE striking faults along which the Pacific plate is moving northwestward with respect to the North America plate (Stock and Hodges, 1989).

The igneous and metamorphic Mesozoic rocks, as well as Tertiary volcanic rocks as young as 12 Ma (San Felipe tuff; Oskin, 2002), and the Hermosillo ignimbrite (Vidal-Solano *et al.*, 2005) are faulted and tilted locally up to 70º to the east (*i.e.*, west of Sierra Kunkaak, north of Bahía Kino). The relation between tilting and continental breakup is clearly evidenced by the deformation of Miocene volcanic rocks, but the structural pattern of the Gulf Extensional Province partially obliterates the previous Basin and Range extensional faulting pattern.

SAMPLING AND ANALYTICAL METHODS

To shed ligth on the crystallization and cooling history of granitoids from the CSB, six samples were collected in the southern area between the northern area of Punta Chueca and Kino Nuevo, and three samples in the northern area, from Punta Tepopa to Rancho Doble I (Figure 2). Three samples of the southern area are aligned along a NE-SW section, perpendicular to the direction of tilting. Eight of these samples were dated by U-Pb zircon geochronology, and three samples of the southern area were also dated by the $^{40}Ar/^{39}Ar$ method in biotite and K-feldspar separates. A whole rock sample of the Tordillo andesite (sample KI-04-08) was dated by the K-Ar method.

For each sample, 1–2 kg of fresh rock chips were collected. Samples were prepared using standard separation techniques, including magnetic separation and heavy liquids. For the U-Pb analysis, zircon crystals were separated by hand-picking under a binocular microscope, for subsequent epoxy mounting and polishing.

Single zircon crystals were analyzed in polished grain mounts with a VG Isoprobe multi-collector ICP-MS equipped with nine Faraday collectors, an axial Daly detector, and four ion-counting channels (Gehrels *et al*., 2006). The Isoprobe is equipped with an ArF Excimer laser, which has an emission wavelength of 193 nm. The analyses were conducted on 50–35 micron spots with an output energy of ~32 mJ and a repetition rate of 10 Hz. Each analysis consisted of a background measurement (one 20-seconds integration on peaks with no laser firing) and twenty 1-second integrations on peaks with the laser firing. Any Hg contribution to the ^{204}Pb mass was accordingly removed by subtracting the background values. The depth of each ablation pit was ~20 microns. Total measurement time was ~90 s per analysis.

The collectors were configured for simultaneous measurement of ^{204}Pb in an ion-counting channel and ^{206}Pb, ^{207}Pb, ^{208}Pb, ^{232}Th, and ^{238}U in Faraday detectors. Inter-element fractionation was monitored by analyzing fragments of SL-1, a large concordant zircon crystal from Sri Lanka (SL-1) with a known (ID-TIMS) age of 564 ± 4 Ma (2 sigma) obtained by George Gehrels (unpublished data). The reported U-Pb ages are based entirely on $^{206}Pb/^{238}U$ ratios because the errors of the $^{207}Pb/^{235}U$ and $^{207}Pb/^{206}Pb$ ratios were too large. This is due primarily to the low intensity (commonly <0.5 mV) of the ^{207}Pb signal from these young, low-U grains. The $^{206}Pb/^{238}U$ ratios were corrected for common Pb by using the measured $^{206}Pb/^{204}Pb$, a common Pb composition from Stacey and Kramers (1975), and an uncertainty of ±1.0 on the common $^{206}Pb/^{204}Pb$.

For each sample, the weighted mean of ~20–25 individual analyses was calculated according to Ludwig (2003). The measurement error was added quadratically to the systematic errors, which include contributions from the calibration correction, decay constant, age of the calibration standard, and composition of common Pb. The systematic errors are 1–2% for these samples. All the U-Pb zircon ages are reported at the 2-sigma level.

Biotite and K-feldspar mineral separates were dated by $^{40}Ar/^{39}Ar$ furnace step-heating and total fusion methods. The mineral concentrates ranged in size between 250 and 180 μm and were obtained to a purity of >99% using heavy liquids and hand-picking techniques. Samples were washed in acetone, alcohol, and deionised water in an ultrasonic cleaner to remove dust and then re-sieved to <180 μm.

Aliquots of biotite and K-feldspar for the different granitic samples were packaged in copper and sealed under vacuum in quartz tubes. The samples were then irradiated in package number KD38 for 5 hours in the central thimble facility at the TRIGA nuclear reactor (GSTR) at the U.S. Geological Survey in Denver, Colorado. The monitor mineral used in the package was Fish Canyon Tuff sanidine (FCT-3) with a K-Ar age of 27.79 Ma (Kunk *et al*., 1985; Cebula *et al*., 1986) relative to MMhb-1 with a K-Ar age of 519.4 ± 2.5 Ma (Alexander *et al*., 1978; Dalrymple *et al*., 1981). The type of container and the geometry of sample and standards are similar to those described by Snee *et al*. (1988).

The samples were analyzed at the U.S. Geological Survey Thermochronology Laboratory in Denver, Colorado, by the $^{40}Ar/^{39}Ar$ furnace step-heating and total fusion dating methods with a MAP 216 mass spectrometer fitted with an electron multiplier. Biotite aliquots were fused in the furnace in a single heating step at ~1,450°C to produce a total fusion age. For additional information on the analytical procedure, see Iriondo *et al*. (2003, 2004).

The argon isotopic data, reported at the 1σ level of analytical precision, were reduced using the computer program Mass Spec (Deino, 2001). We used the decay constants recommended by Steiger and Jäger (1977). Table 4 shows $^{40}Ar/^{39}Ar$ furnace step-heating and total fusion data and includes the identification of individual temperature steps, plateau, average, and total gas ages. An individual step age

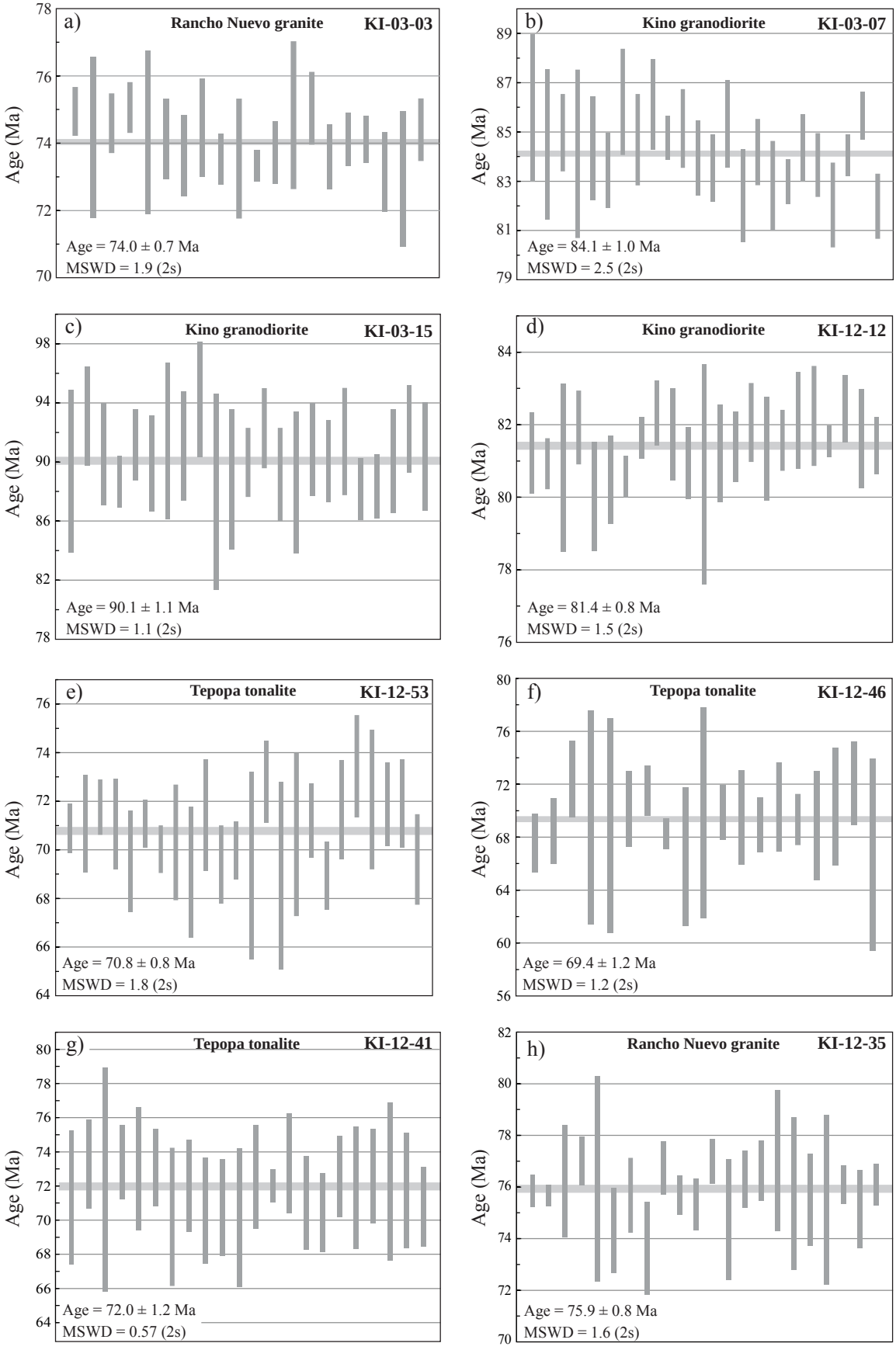

Figure 4. ^{206}Pb-^{238}U zircon ages for samples of the Coastal Sonora batholith. South zone samples (a, b, c and d) and north zone samples (e, f, g and h).

Table 1. Summary of U/Pb dated samples of the coastal Sonora batholith, Mexico.

Sample	Latitude N	Longitude W	Unit	Ages (Ma)
South zone / Kino Nuevo – Punta Chueca				
KI-03-03	402750	3198692	Rancho Nuevo granite	74.0 ± 0.7
KI-03-07	399405	3194133	Kino granodiorite	84.1 ± 1.0
KI-03-15	408084	3202328	Kino granodiorite	90.1 ± 1.1
KI-12-12	391513	3209999	Kino granodiorite	81.4 ± 0.8
KI-12-53	387368	3214508	Tepopa tonalite	70.8 ± 1.8
North zone / Punta Chueca – Punta Tepopa				
KI-12-35	387066	3238468	R. Nuevo granite (foliated)	75.9 ± 0.8
KI-12-41	380900	3244078	Tepopa tonalite	72.0 ± 1.2
KI-12-46	365796	3247634	Tepopa tonalite	69.4 ± 1.2

Note: Dated at Isotope Geochemistry Laboratory University of Arizona in Tucson, USA. The coordinates are UTM, datum WGS 84.

represents the apparent age obtained for a single temperature step analysis. A plateau age (not present for these samples) is identified when three or more contiguous steps in the age spectrum agree in age, within the limits of analytical precision, and contain more than 50% of the $^{39}Ar_K$ released from the sample (Fleck *et al.*, 1977). Total gas ages represent the age calculated from the integration of all the $^{40}Ar/^{39}Ar$ step-heating age results for the sample into one single age value; the total gas ages are thus roughly equivalent to conventional K-Ar ages. No analytical precision is calculated for the total gas age because this analytical uncertainty in many cases does not represent the total geological uncertainty in the age of the mineral and/or rock.

GEOCHRONOLOGY RESULTS

Most of the dated samples are granodiorite-tonalite to granite (Table 1), generally with coarse to very coarse-grained textures, and large phenocrysts of K-feldspar. Zircons separated from all the samples have the well defined crystallographic forms, with well-developed and preserved faces, that characterize igneous zircons (Pupin, 1983). The absence of inherited zircon is indicated by the low dispersion in the distribution of the calculated ages of the samples (Figure 4), which yielded only Cretaceous ages (from 90.1 ± 1.1 to 69.4 ± 1.1 Ma). This result is supported by the $^{40}Ar/^{39}Ar$ ages obtained in biotite, which are also Late Cretaceous (from 66.95 ± 0.28 to 73.61 ± 0.12 Ma), suggesting a regional cooling below the biotite closure temperature at this time (rough closure temperature estimate for biotite: ~300±40 °C; *e.g.*, McDougall and Harrison, 1999). The description of the geochronological results was separated in two zones (north and south), based on their geographic location. Geochronological data are presented on Tables 1- 4.

Southern area

Three samples were collected along a 9 km long NE-SW transect between Kino Nuevo and the northern Punta Chueca (Figure 2). The units sampled are the Kino granodiorite close to the shoreline (KI-03-07), the Rancho Nuevo granite (KI-03-03) in the middle and, to the east, the Kino granodiorite (KI-03-15). The samples collected to the east and north of Punta Chueca are: Kino granodiorite (KI-12-12) and Tepopa tonalite (KI-12-53). A sample of the Tordillo andesite was collected north of Kino Nuevo (KI-04-08). The five intrusive samples were dated by U-Pb, three of them were also dated by $^{40}Ar/^{39}Ar$, while the andesite sample was dated by the K-Ar method.

The three ^{206}Pb-^{238}U zircon ages obtained for the Kino granodiorite are consistent with each other, indicating that crystallization occurred in Late Cretaceous time, between 90.1 ± 1.1 and 81.4 ± 0.8 Ma (Figure 4; Table 1). Younger crystallization ages of the Rancho Nuevo granite (74.0 ± 0.7 Ma) and the Tepopa tonalite (70.8 ± 1.8 Ma) are consistent with field relations showing that the Rancho Nuevo granite and Tepopa tonalite intruded the Kino granodiorite. The older sample of the Kino granodiorite (KI-03-15) shows ductile deformation whereas the younger samples (KI-03-07 and KI-12-12) are unaffected by this deformation, perhaps indicating that the intrusion began under syntectonic conditions. The youngest sample (KI-12-53) could represent the beginning of a tendency to younger ages to the north of the CSB.

The three samples of the NE-SW section (KI-03-03, KI-03-07 and KI-03-15) were also dated by ^{40}Ar-^{39}Ar geochronology to determine their thermal history between ~300°C (±40) and ~150°C (±40), the rough estimate for closure temperatures of biotite and low-temperature K-feldspar domains, respectively.

Biotite from the Rancho Nuevo granite (KI-03-03) yielded a total fusion age of 66.95 ± 0.28 Ma (Figure 5a and Table 4) that we interpret as the best approximation for the timing of cooling of the granite below ~300°C (±40). However, the reliability of this age is poor because of the low percentage of radiogenic $^{40}Ar^*$ (31%), which may be explained by the alteration of biotite to chlorite. The K-feldspar analysis yielded an age range of cooling between 62.8 and ~60 Ma. We interpret that the upper age represents the K-feldspar domains with higher argon retention [rough estimate of high temperature K-feldspar closure temperature: ~250°C (±40)], whereas the lower end represents the feldspar domains with lower retention properties (rough estimate of low temperature K-feldspar closure temperature: ~150°C (± 40). These cooling ages combined with the zircon crystallization age of 74.0 ± 0.7 Ma indicate a relatively slow initial cooling through biotite and a slower cooling between biotite and low-T K-feldspar (Figure 6).

Kino granodiorite biotite sample KI-03-07 yielded a single step age of 72.41 ± 0.22 Ma (Table 4) that represents the time of cooling below biotite closure. The age

spectrum for K-feldspar (Figure 5b) shows a large age gradient between 63 and 41.5 Ma implying a significantly slower cooling rate than that of Rancho Nuevo granite, although cooling in the early stages, between zircon (84.1 ± 1.0 Ma) and biotite, is slightly slower than for Rancho Nuevo granite sample (Figure 6). A second Kino granodiorite sample (KI-03-15) was dated on a biotite separate that yielded a single-step age of 73.61 ± 0.12 Ma (Table 4). The age spectrum for the K-feldspar of this sample (Figure 5c and Table 4) displays a gradient between 68.4 and 59.5 Ma. The cooling curve for this last granodiorite sample indicate an intermediate cooling rate with respect to the

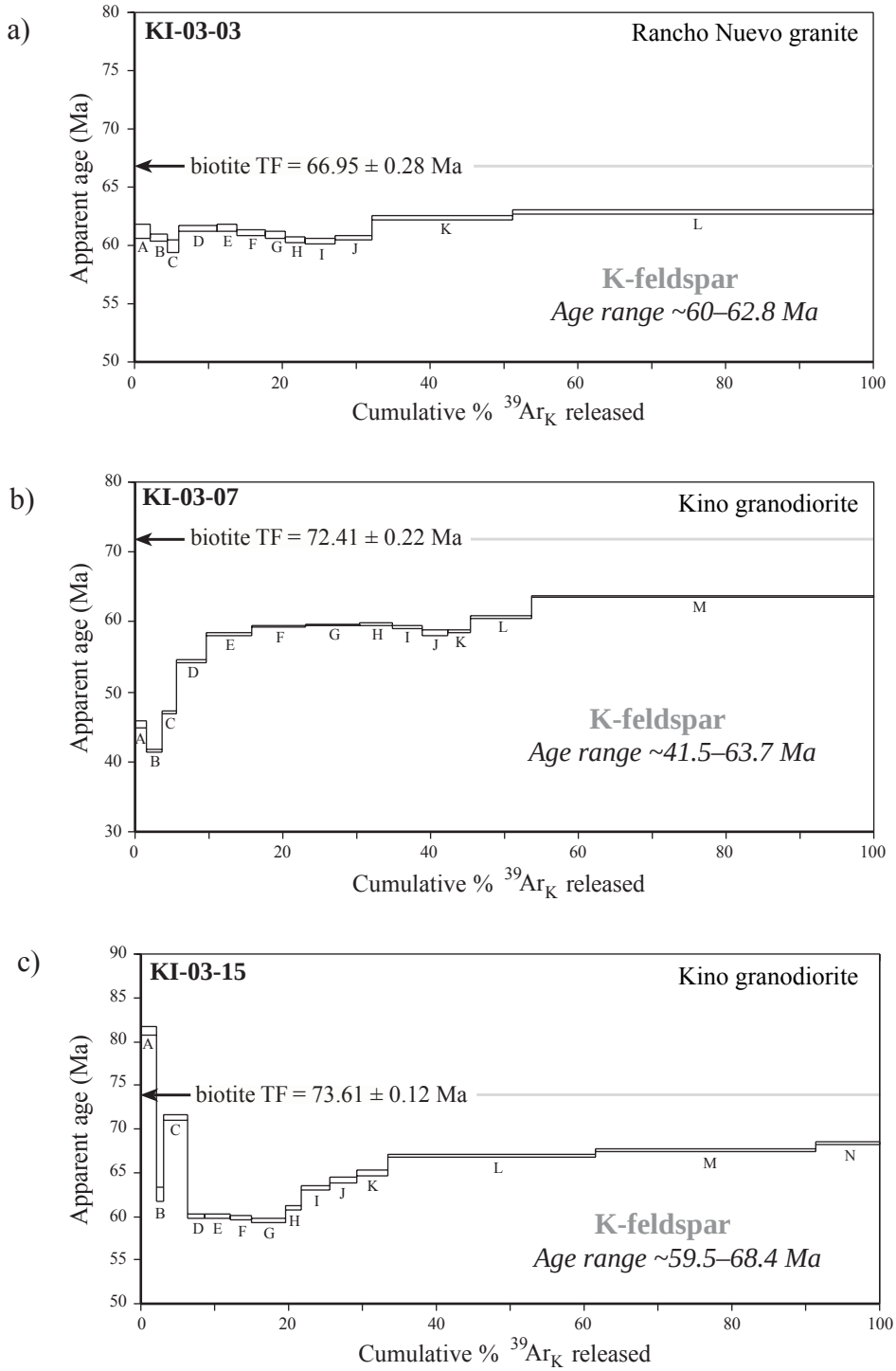

Figure 5. Results of $^{40}Ar/^{39}Ar$ dating of samples from the southern zone. Furnace step-heating spectra and estimated age ranges for K-feldspars. Apparent ages in the diagrams are plotted at the 2σ level of precision to improve visual assessment of the data. Also shown are ages obtained by total fusion (TF) of biotites.

Table 2. Summary of $^{40}Ar/^{39}Ar$ and K/Ar dated samples from the Coastal Sonora batholith, México.

Sample	Latitude N	Longitude W	Unit	Ages (Ma)		
				$^{40}Ar/^{39}Ar$ (Biotite)	$^{40}Ar/^{39}Ar$ (K-feldsp.)	K-Ar (WR)
South zone / Kino Nuevo – Punta Chueca						
KI-03-03	402750	3198692	R. Nuevo Granite	66.95 ± 0.28	~60 ± 62.8	
KI-03-07	399405	3194133	Kino Granodiorite	72.41 ± 0.22	41.5 - 63.7	
KI-03-15	408084	3202328	Kino Granodiorite	73.61 ± 0.12	59.5 - 68.4	
KI-04-08	400894	3202605	Tordillo Andesite			62.5 ± 1.5

previously described samples. Appartently, the older Kino granodiorite samples KI-03-15 and KI-03-07 needed more time to cool below K-feldspar closure, perhaps because the younger pulse of magmatism (Rancho Nuevo granite) created a regional thermal gradient that maintained the preexisting rocks above their closure temperatures for the Ar-Ar geochronometers. The Rancho Nuevo granite sample (KI-03-03) cooled relatively rapidly and was not affected by any significant thermal pulse since cooling below K-feldspar closure [low retention domains at ~150°C (±40) around 60 Ma (Figure 6)].

The Tordillo andesite (KI-04-08) yielded a K-Ar whole rock age of 62.5 ± 1.5 Ma (Table 2). The emplacement of this unit occurred at the time the Kino granodiorite and Rancho Nuevo granite cooled through ~250°C (±40), the rough estimate for closure temperature of the high-retention domains of K-feldspar. The age of the Tordillo andesite is similar to other ages obtained further to the east, in andesites of the Tarahumara Formation (McDowell *et al*., 2001; Roldán-Quintana, 2002), suggesting that the Cretaceous-Paleogene volcanic activity related to the Laramide magmatic arc was not restricted to central Sonora but was also present along the western margin of the North America craton. We interpret the scarcity of outcrops of the Tarahumara Formation in western Sonora as a result of the intense uplift and subsequent erosion during Basin and Range faulting and pre-Gulf rifting.

Northern area

In the area between Rancho Doble I and Punta Tepopa, three samples were collected and dated by U-Pb zircon geochronology (Figure 2). ^{206}Pb-^{238}U zircon ages of the three samples correspond to Late Cretaceous crystallization, varying between 75.9 ± 0.8 and 69.4 ± 1.2 Ma (Table 1). They are distinctly younger than the Kino granodiorite in the southern area.

Sample KI-12-46 belongs to the Isla Tiburón-Punta Tepopa range, whereas the other two samples belong to the Kunkaak range (Figure 2). Sample KI-12-35 is part of the Rancho Nuevo granite and corresponds to a porphyric monzogranite, which presents a clear magmatic foliation. Samples KI-12-46 and KI-12-41 belong to the Tepopa tonalite, which is older than the granite, based on intrusion relationships from several localities.

The KI-12-35 sample is the oldest one, with a zircon ^{206}Pb-^{238}U age of 75.9 ± 0.8 Ma, and corresponds to the zone of magmatic foliation of the Rancho Nuevo granite near the intrusive contact with the Kino granodiorite. This age is in agreement with the age obtained in the southern area (KI-03-03), also intruding the Kino granodiorite.

Samples of the Tepopa tonalite (KI-12-41 and KI-12-46) yield similar ^{206}Pb-^{238}U ages that are in close agreement with that obtained for the Tepopa tonalite (70.8 ± 1.8 Ma) from the southern zone. With these results we can conclude that the Tepopa tonalite was emplaced in an time interval of about 3 Ma, and is the last intrusive unit of the CSB.

DISCUSSION

Crystallization and cooling of the Sonora coastal batholith

Petrological characteristics and ^{206}Pb-^{238}U zircon ages indicate that the CSB consists of several granitoid complexes that crystallized during Late Cretaceous, between ~90 and 70 Ma (Figure 6). The CSB was emplaced in the continental active margin of North America, in a region characterized by the transition between two previously juxtaposed basements; a northern one related to the margin of the North America craton, and a southern one with oceanic basin affinities since the Paleozoic time (Valencia-Moreno *et al*., 2001). Nevertheless, the lack of inherited zircon in the analyzed samples does not provide any complementary information about the nature of the basement in which the CSB intruded in the studied area (Figure 4). Although the selection of individual zircon crystals was made by hand-picking, it is unlikely that this procedure has induced a lack of inherited zircons in all samples.

The crystallization of the CSB began with the Puerto Rico diorite (not dated), emplaced as small bodies around ~90 Ma. Later, between ~90 and ~80 Ma, the Kino granodiorite was emplaced within a relatively cold Puerto Rico diorite; this is interpreted by the sharp and regular contacts that could be related to a relatively shallow level of emplacement. The weak ductile deformation observed in the locality of sample KI-03-15 (Figure 2) is correlated to local processes during the cooling of the pluton, because

Table 3. U-Pb results, the errors are reported to 1-sigma level.

Spot	U (ppm)	Th (ppm)	U/Th	$^{206}Pb/^{204}Pbc$	$^{206}Pb/^{238}U$ ratio	±(%)	$^{206}Pb/^{238}U$ age	±(Ma)
KI-03-03								
1	879	406	2.2	1562	0.01169	0.97	74.9	0.7
2	314	339	0.9	569	0.01157	3.24	74.2	2.4
3	919	412	2.2	2247	0.01164	1.19	74.6	0.9
4	840	305	2.8	2214	0.01171	1.01	75.1	0.8
5	478	194	2.5	663	0.01160	3.27	74.3	2.4
6	372	185	2.0	838	0.01157	1.62	74.1	1.2
7	1386	706	2.0	3074	0.01149	1.64	73.6	1.2
8	477	207	2.3	1829	0.01162	1.97	74.4	1.5
9	268	154	1.7	1535	0.01147	1.04	73.5	0.8
10	298	158	1.9	387	0.01147	2.43	73.5	1.8
11	556	210	2.6	2044	0.01144	0.64	73.3	0.5
12	456	228	2.0	772	0.01150	1.27	73.7	0.9
13	233	106	2.2	703	0.01168	2.94	74.8	2.2
14	527	291	1.8	1458	0.01171	1.44	75.0	1.1
15	1046	495	2.1	3402	0.01148	1.31	73.6	1.0
16	795	304	2.6	1657	0.01156	1.08	74.1	0.8
17	878	625	1.4	2428	0.01156	0.95	74.1	0.7
18	737	338	2.2	2264	0.01141	1.62	73.2	1.2
19	210	115	1.8	360	0.01138	2.77	72.9	2.0
20	505	286	1.8	1662	0.01161	1.25	74.4	0.9
KI-03-07								
1	177	99	1.8	439	0.01343	3.48	86.0	3.0
2	231	144	1.6	483	0.01319	3.63	84.5	3.0
3	431	250	1.7	1173	0.01327	1.85	85.0	1.6
4	186	99	1.9	585	0.01313	4.09	84.1	3.4
5	292	130	2.2	456	0.01317	2.50	84.3	2.1
6	348	203	1.7	588	0.01303	1.83	83.4	1.5
7	316	181	1.7	1063	0.01346	2.51	86.2	2.2
8	344	210	1.6	1049	0.01322	2.20	84.7	1.9
9	432	239	1.8	1069	0.01345	2.14	86.1	1.8
10	446	253	1.8	1343	0.01324	1.06	84.8	0.9
11	497	368	1.4	1302	0.01329	1.88	85.1	1.6
12	544	353	1.5	1326	0.01311	1.82	84.0	1.5
13	512	245	2.1	1443	0.01304	1.64	83.5	1.4
14	307	159	1.9	1333	0.01332	2.09	85.3	1.8
15	289	178	1.6	713	0.01287	2.30	82.4	1.9
16	345	188	1.8	730	0.01314	1.60	84.2	1.3
17	424	212	2.0	813	0.01293	2.20	82.8	1.8
18	337	194	1.7	792	0.01295	1.11	83.0	0.9
19	310	169	1.8	1108	0.01317	1.62	84.3	1.4
20	421	239	1.8	873	0.01306	1.55	83.7	1.3
21	330	168	2.0	691	0.01281	2.10	82.0	1.7
22	557	285	2.0	1839	0.01312	1.01	84.0	0.8
23	314	203	1.5	777	0.01337	1.13	85.6	1.0
24	296	185	1.6	700	0.01280	1.62	82.0	1.3
KI-03-15								
1	104	104	1.0	202	0.01396	6.20	89.3	5.5
2	90	67	1.3	334	0.01455	3.61	93.1	3.3
3	109	97	1.1	341	0.01414	3.83	90.5	3.4
4	189	175	1.1	654	0.01385	1.98	88.7	1.7
5	115	112	1.0	471	0.01424	2.66	91.2	2.4
6	124	90	1.4	438	0.01404	3.61	89.9	3.2
7	87	66	1.3	261	0.01428	5.82	91.4	5.3
8	104	88	1.2	378	0.01422	4.09	91.1	3.7
9	90	70	1.3	495	0.01472	4.17	94.2	3.9
10	71	42	1.7	307	0.01374	7.60	88.0	6.6
11	68	52	1.3	260	0.01387	5.36	88.8	4.7
12	105	90	1.2	363	0.01405	2.62	90.0	2.3
13	99	77	1.3	599	0.01442	2.95	92.3	2.7
14	97	101	1.0	285	0.01393	3.55	89.2	3.1
15	123	132	0.9	459	0.01384	5.43	88.6	4.8
16	108	108	1.0	271	0.01419	3.49	90.8	3.1
17	121	77	1.6	338	0.01407	3.09	90.1	2.8
18	100	75	1.3	465	0.01428	4.00	91.4	3.6
19	160	122	1.3	445	0.01377	2.39	88.2	2.1
20	367	179	2.0	1151	0.01380	2.47	88.3	2.2
21	95	78	1.2	304	0.01406	3.92	90.0	3.5
22	111	74	1.5	570	0.01441	3.24	92.2	3.0
23	108	99	1.1	371	0.01412	4.09	90.4	3.7

Table 3 (continued). U-Pb results, the errors are reported to 1-sigma level.

Spot	U (ppm)	Th (ppm)	U/Th	$^{206}Pb/^{204}Pbc$	$^{206}Pb/^{238}U$ ratio	±(%)	$^{206}Pb/^{238}U$ age	±(Ma)
KI-12-12								
1	620	313	2.0	1232	0.01268	1.39	81.2	1.1
2	453	267	1.7	837	0.01263	0.87	80.9	0.7
3	220	98	2.3	930	0.01261	2.88	80.8	2.3
4	658	249	2.6	1090	0.01279	1.25	81.9	1.0
5	315	214	1.5	694	0.01249	1.89	80.0	1.5
6	550	360	1.5	615	0.01256	1.52	80.5	1.2
7	990	472	2.1	1212	0.01257	0.71	80.6	0.6
8	1217	1053	1.2	2930	0.01275	0.71	81.6	0.6
9	696	267	2.6	1191	0.01285	1.09	82.3	0.9
10	783	276	2.8	1394	0.01276	1.55	81.7	1.3
11	688	206	3.3	1134	0.01264	1.23	80.9	1.0
12	171	49	3.5	470	0.01259	3.78	80.6	3.0
13	420	139	3.0	998	0.01268	1.67	81.2	1.3
14	825	277	3.0	1933	0.01271	1.20	81.4	1.0
15	720	331	2.2	1769	0.01281	1.34	82.1	1.1
16	336	171	2.0	896	0.01270	1.76	81.3	1.4
17	677	269	2.5	1013	0.01273	1.04	81.6	0.8
18	713	304	2.3	1692	0.01282	1.64	82.1	1.3
19	881	310	2.8	1447	0.01284	1.69	82.2	1.4
20	871	312	2.8	1977	0.01273	0.54	81.5	0.4
21	1055	492	2.1	2278	0.01287	1.13	82.4	0.9
22	740	301	2.5	935	0.01274	1.69	81.6	1.4
23	781	271	2.9	958	0.01271	0.98	81.4	0.8
KI-12-53								
1	343	194	1.8	960	0.01105	1.45	70.9	1.0
2	242	110	2.2	604	0.01109	2.83	71.1	2.0
3	397	145	2.7	1122	0.01119	1.60	71.7	1.1
4	209	85	2.5	629	0.01108	2.63	71.1	1.9
5	265	127	2.1	1109	0.01084	3.01	69.5	2.1
6	255	116	2.2	1155	0.01109	1.39	71.1	1.0
7	211	72	2.9	967	0.01092	1.41	70.0	1.0
8	205	119	1.7	791	0.01096	3.40	70.3	2.4
9	221	113	2.0	353	0.01077	3.90	69.1	2.7
10	214	105	2.0	871	0.01114	3.24	71.4	2.3
11	278	132	2.1	1056	0.01082	2.33	69.4	1.6
12	315	188	1.7	840	0.01091	1.71	70.0	1.2
13	216	111	1.9	422	0.01081	5.58	69.3	3.9
14	222	86	2.6	929	0.01136	2.32	72.8	1.7
15	105	33	3.1	331	0.01075	5.62	68.9	3.9
16	222	98	2.3	346	0.01102	4.78	70.6	3.4
17	477	211	2.3	1347	0.01111	2.15	71.2	1.5
18	240	138	1.7	814	0.01075	2.04	68.9	1.4
19	411	172	2.4	1923	0.01118	2.86	71.6	2.0
20	338	220	1.5	1651	0.01146	2.89	73.4	2.1
21	192	87	2.2	778	0.01124	4.00	72.1	2.9
22	390	221	1.8	1907	0.01121	2.39	71.9	1.7
23	212	117	1.8	596	0.01121	2.53	71.9	1.8
24	375	212	1.8	681	0.01085	2.68	69.6	1.9
KI-12-46								
1	190	115	1.7	419	0.01053	3.33	67.5	2.2
2	202	97	2.1	325	0.01067	3.64	68.4	2.5
3	155	72	2.1	542	0.01129	4.01	72.4	2.9
4	53	24	2.2	130	0.01083	11.65	69.5	8.1
5	40	24	1.7	127	0.01074	11.82	68.9	8.1
6	124	64	1.9	442	0.01094	4.12	70.1	2.9
7	227	97	2.3	1027	0.01115	2.65	71.5	1.9
8	269	105	2.5	751	0.01065	1.71	68.3	1.2
9	84	43	2.0	267	0.01037	7.89	66.5	5.2
10	50	26	1.9	242	0.01089	11.45	69.9	8.0
11	208	99	2.1	707	0.01090	2.97	69.9	2.1
12	155	83	1.9	350	0.01084	5.16	69.5	3.6
13	313	154	2.0	633	0.01075	2.99	68.9	2.0
14	112	67	1.7	438	0.01096	4.82	70.3	3.4
15	260	113	2.3	653	0.01081	2.81	69.3	1.9
16	63	47	1.4	219	0.01074	5.98	68.9	4.1
17	97	39	2.5	294	0.01097	6.34	70.3	4.4
18	169	34	5.0	555	0.01124	4.37	72.1	3.1
19	45	20	2.2	150	0.01040	10.88	66.7	7.2
20	94	93	1.0	436	0.01376	5.91	88.1	5.2

Table 3 (continued). U-Pb results, the errors are reported to 1-sigma level.

Spot	U (ppm)	Th (ppm)	U/Th	$^{206}Pb/^{204}Pbc$	$^{206}Pb/^{238}U$ ratio	±(%)	$^{206}Pb/^{238}U$ age	±(Ma)
KI-12-41								
1	78	65	1.2	315	0.01113	5.53	71.3	3.9
2	432	696	0.6	890	0.01143	3.57	73.3	2.6
3	64	27	2.3	184	0.01129	9.12	72.4	6.6
4	233	175	1.3	642	0.01145	2.96	73.4	2.2
5	150	97	1.6	249	0.01139	4.96	73.0	3.6
6	159	81	2.0	596	0.01140	3.11	73.1	2.3
7	128	90	1.4	584	0.01095	5.79	70.2	4.0
8	148	76	2.0	497	0.01123	3.76	72.0	2.7
9	141	61	2.3	607	0.01101	4.44	70.6	3.1
10	118	69	1.7	185	0.01104	4.00	70.7	2.8
11	133	100	1.3	371	0.01094	5.81	70.1	4.1
12	322	236	1.4	793	0.01131	4.21	72.5	3.0
13	420	243	1.7	1443	0.01123	1.34	72.0	1.0
14	173	144	1.2	413	0.01144	3.99	73.3	2.9
15	134	84	1.6	280	0.01107	3.86	71.0	2.7
16	158	89	1.8	414	0.01099	3.29	70.5	2.3
17	193	129	1.5	696	0.01132	3.29	72.5	2.4
18	145	85	1.7	381	0.01121	4.99	71.9	3.6
19	113	60	1.9	240	0.01132	3.83	72.6	2.8
20	109	55	2.0	309	0.01127	6.43	72.3	4.6
21	153	103	1.5	567	0.01119	4.73	71.7	3.4
22	168	113	1.5	330	0.01104	3.31	70.8	2.3
KI-12-35								
1	512	273	1.9	410	0.01183	0.83	75.8	0.6
2	707	250	2.8	726	0.01181	0.55	75.7	0.4
3	436	203	2.2	250	0.01189	2.87	76.2	2.2
4	573	184	3.1	1558	0.01202	1.22	77.0	0.9
5	74	33	2.2	167	0.01191	5.24	76.3	4.0
6	289	181	1.6	436	0.01160	2.23	74.3	1.7
7	655	370	1.8	967	0.01181	1.93	75.7	1.5
8	501	205	2.4	286	0.01148	2.46	73.6	1.8
9	350	235	1.5	942	0.01197	1.34	76.7	1.0
10	769	346	2.2	2369	0.01181	1.00	75.7	0.8
11	439	236	1.9	811	0.01175	1.33	75.3	1.0
12	570	262	2.2	1500	0.01201	1.12	77.0	0.9
13	175	108	1.6	322	0.01166	3.15	74.7	2.3
14	430	286	1.5	863	0.01190	1.46	76.3	1.1
15	309	162	1.9	800	0.01196	1.53	76.6	1.2
16	197	89	2.2	488	0.01202	3.55	77.0	2.7
17	197	78	2.5	225	0.01182	3.92	75.7	3.0
18	1041	704	1.5	929	0.01178	2.37	75.5	1.8
19	110	43	2.5	400	0.01178	4.36	75.5	3.3
20	407	191	2.1	1606	0.01187	0.99	76.1	0.7
21	411	211	1.9	1376	0.01173	2.03	75.2	1.5
22	566	222	2.5	1630	0.01187	1.07	76.1	0.8

such deformation was not observed in other samples. The Rancho Nuevo granite and granitic dikes were emplaced at around ~76–74 Ma. The youngest units on the studied area corresponds to the Tepopa tonalite, emplaced between 72 and 69 Ma, and the Tordillo andesite emplaced at ~62.5 Ma (Table 1). While the volcanics are spatially related to the Kino granodiorite, our geochronologic results demonstrate that the bodies are not coeval.

The U-Pb isotopic zircon ages obtained for the Kino granodiorite, Tepopa tonalite and Rancho Nuevo granite display a clear difference in crystallization age (Figure 2). The U-Pb ages reported in this study are older than U-Pb zircon ages obtained by Anderson *et al*. (1980) in the Sierra Mazatán and Puerto del Sol (57 ± 3 and 58 ± 3 Ma), and by Poole *et al*. (1991) in Barita de Sonora mining district (62.0 ± 1 Ma). Furthermore, these U-Pb ages are older and younger than ages obtained by Anderson *et al*. (1980) to the north in the Sierra Guacomea and Rancho Los Alamos (74 ± 2 and 78 ± 3 Ma, respectively). The correlation between the U-Pb ages from this and previous studies shows a tendency for the crystallization ages to be younger to the east, toward the interior of Sonora. This tendency supports the idea of an eastward magmatic migration during the Laramide orogeny (Damon *et al*., 1983b).

$^{40}Ar/^{39}Ar$ and K-Ar ages obtained in this study agree with previous K-Ar and $^{40}Ar/^{39}Ar$ results (Gastil and Krummenacher, 1977; Mora-Alvarez, 1992, and Valencia-Moreno *et al*., 2006) for the central part of the CSB and Isla Tiburón. North of the study area, near Puerto Libertad, Gastil and Krummenacher (1977) re-

Table 4. $^{40}Ar/^{39}Ar$ furnace step-heating (K-feldspar) and total fusion data (biotite).

Step	Temp. ºC	% ^{39}Ar of total	Radiogenic yield (%)	$^{39}Ar_k$ (Moles)	$^{40}Ar/^{39}Ar_k$	Apparent K/Ca	Apparent K/Ca	Apparent age (Ma)	Error (Ma)
KI-03-15 *Sonora* ***K-feldspar*** J = 0.001278 ± 0.50% wt = 4.3 mg #22KD38									
A	950	2.1	65.7	6.57E-15	36.034	b.d.l.	3.1	81.22	± 0.22
B	1000	0.9	79.0	2.72E-15	27.576	b.d.l.	15.5	62.48	± 0.43
C	1050	3.3	65.6	1.03E-14	31.561	b.d.l.	9.3	71.34	± 0.18
D	1100	2.3	87.6	7.04E-15	26.479	b.d.l.	29.9	60.04	± 0.13
E	1150	3.5	80.2	1.09E-14	26.463	b.d.l.	30.3	60.00	± 0.14
F	1200	3.0	69.0	9.26E-15	26.384	b.d.l.	27.9	59.83	± 0.15
G	1250	4.5	71.2	1.39E-14	26.235	b.d.l.	22.7	59.50	± 0.13
H	1275	2.2	78.0	6.71E-15	26.904	b.d.l.	21.3	60.99	± 0.14
I	1300	3.9	71.9	1.21E-14	27.914	b.d.l.	17.9	63.24	± 0.13
J	1325	3.6	70.7	1.12E-14	28.303	b.d.l.	6.3	64.10	± 0.15
K	1350	4.2	69.6	1.30E-14	28.701	b.d.l.	2.0	64.99	± 0.15
L	1400	28.1	77.4	8.71E-14	29.560	b.d.l.	15.2	66.90	± 0.10
M	1500	29.7	77.3	9.23E-14	29.867	b.d.l.	18.0	67.58	± 0.10
N	1650	8.7	77.5	2.71E-14	30.214	b.d.l.	15.9	68.35	± 0.11
							Total gas age = 66.25		
KI-03-15 *Sonora* ***biotite total fusion*** J = 0.001270 ± 0.50% wt = 1.2 mg #10KD38									
A	1450	100	76.1	6.21E-14	32.791	b.d.l.	2.91	73.61	± 0.12
KI-03-07 *Sonora* ***K-feldspar*** J = 0.001277 ± 0.50% wt = 3.9 mg #17KD38									
A	950	1.5	81.4	4.13E-15	19.938	b.d.l.	1.0	45.36	± 0.25
B	1000	2.2	92.1	6.16E-15	18.230	b.d.l.	37.4	41.52	± 0.10
C	1050	1.8	96.6	5.02E-15	20.714	b.d.l.	45.4	47.10	± 0.12
D	1100	4.2	96.4	1.16E-14	23.981	b.d.l.	47.8	54.42	± 0.09
E	1150	6.1	97.8	1.71E-14	25.675	b.d.l.	99.5	58.20	± 0.08
F	1200	7.3	97.8	2.04E-14	26.186	b.d.l.	93.6	59.34	± 0.08
G	1250	7.2	98.0	2.01E-14	26.303	b.d.l.	51.7	59.60	± 0.07
H	1275	4.4	98.0	1.22E-14	26.327	b.d.l.	41.6	59.65	± 0.09
I	1300	4.0	96.6	1.12E-14	26.127	b.d.l.	51.6	59.21	± 0.09
J	1325	3.5	95.1	9.61E-15	25.794	b.d.l.	42.3	58.47	± 0.17
K	1350	3.2	92.4	8.98E-15	25.868	b.d.l.	1.4	58.63	± 0.12
L	1400	8.2	95.7	2.27E-14	26.782	b.d.l.	15.9	60.67	± 0.10
M	1650	46.4	97.1	1.29E-13	28.139	b.d.l.	89.5	63.69	± 0.07
							Total gas age = 60.35		
KI-03-07 *Sonora* ***biotite total fusion*** J = 0.001276 ± 0.50% wt = 1.9 mg #9KD38									
A	1450	100	74.1	2.00E-14	32.094	b.d.l.	6.18	72.41	± 0.22
KI-03-03 *Sonora* ***K-feldspar*** J = 0.001277 ± 0.50% wt = 4.3 mg #21KD38									
A	1000	2.1	65.9	5.27E-15	27.041	b.d.l.	16.4	61.25	± 0.30
B	1050	2.3	75.4	5.75E-15	26.781	b.d.l.	21.8	60.67	± 0.17
C	1100	1.6	84.8	3.88E-15	26.465	b.d.l.	31.1	59.96	± 0.28
D	1150	5.1	83.3	1.26E-14	27.123	b.d.l.	36.1	61.43	± 0.12
E	1200	2.8	86.1	6.86E-15	27.173	b.d.l.	43.7	61.54	± 0.13
F	1250	3.8	83.5	9.43E-15	26.959	b.d.l.	28.9	61.06	± 0.11
G	1275	2.6	87.6	6.50E-15	26.879	b.d.l.	26.0	60.89	± 0.14
H	1300	2.7	84.8	6.72E-15	26.699	b.d.l.	25.0	60.48	± 0.14
I	1325	4.0	82.1	9.98E-15	26.624	b.d.l.	34.5	60.32	± 0.13
J	1350	5.1	78.8	1.27E-14	26.776	b.d.l.	1.6	60.66	± 0.11
K	1400	19.0	86.4	4.71E-14	27.550	b.d.l.	34.4	62.38	± 0.09
L	1650	48.8	87.9	1.21E-13	27.761	b.d.l.	40.0	62.85	± 0.08
							Total gas age = 62.12		
KI-03-03 *Sonora* ***biotite total fusion*** J = 0.001269 ± 0.50% wt = 1.0 mg #15KD38									
A	1450	100	34.6	3.46E-14	29.793	b.d.l.	1.60	66.95	± 0.28

Ages calculated assuming an initial $^{40}Ar/^{36}Ar = 295.5 \pm 0$. All precision estimates are at the one sigma level of precision. Ages of individual steps do not include error in the irradiation parameter J. No error is calculated for the total gas age. b.d.l.= below detection limit for ^{37}Ar.

ported K-Ar ages in biotite and hornblende for intrusive granitoids of the CSB ranging from 70 to 60 Ma. In the region of Guaymas and San Carlos, further to the south, Mora-Alvarez (1992) and Roldán-Quintana (2002) reported K-Ar ages in hornblende between 83.0 ± 2.1 and 82.7 ± 1.7 Ma and in biotite between 81.1 ± 2.8 and 76.9 ± 2.8 Ma, which provides further indication that the CSB exposes older rocks to the south.

The spatial distribution of isotopic ages of plutons in Central Sonora between 30° and 32° N latitude (Figure 7) has been interpreted as evidence of progressive eastward migration of the Cretaceous-Tertiaty magmatic arc (Damon

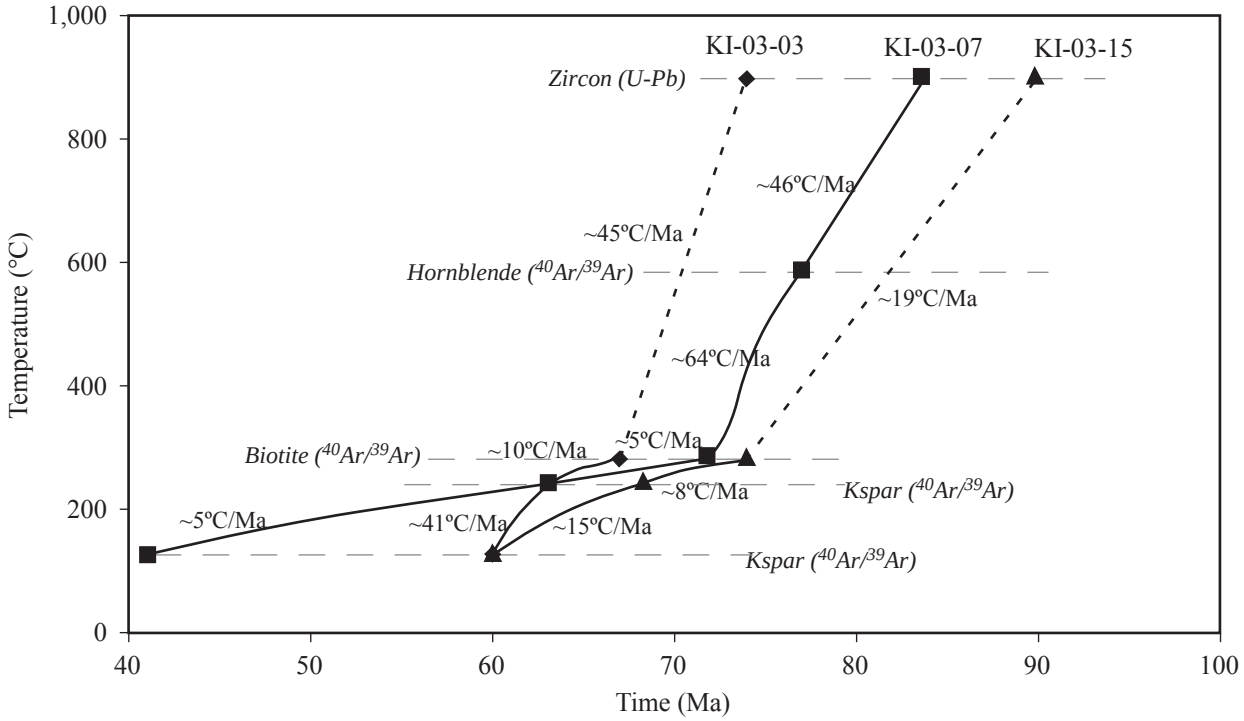

Figure 6. Diagram of the cooling history for the samples of the SE section, to the north of Kino Nuevo. Data of $^{40}Ar/^{39}Ar$ data in hornblende are not available for samples KI-03-03 and KI-03-15; for sample KI-03-07 is correlated from Valencia-Moreno *et al*. (2006).

et al., 1983a). The ages obtained in the present study support this hypothesis for the arc migration. In addition, the isotopic age gradient from south to north within the CSB suggests that the orientation of the arc axis was oblique with respect to the present coastline of Sinaloa and Sonora, which is a morphotectonic feature controlled by the Tertiary history dominated by the Basin and Range extension and the opening of the Gulf of California.

We suggest that some zones exist, as the CSB, with a local magmatic evolution that does not follow the general chronological evolution and migration pattern of the entire magmatic arc. In the case of CSB, the magmatism remained static for about of 10 to 20 Ma, which is suggested by the geochemical magmatic differentiation from diorite to granite emplaced at the same place.

Correlation of the CSB with the Peninsular Ranges Batholith

The correlation of the batholiths located on both sides of the Gulf of California has been addressed by several authors (*e.g.*, Gastil and Krummenacher, 1977), and is supported by similar chemical, petrographic and geochronological characteristics (*e.g.*, Schaaf *et al*., 2000). Ages of granitoid rocks dated in the eastern margin of the Baja California peninsula support this interpretation: for example 78.4 ± 2.9 Ma K-Ar (McFall, 1968) and 99 ± 2 Ma (Ledesma-Vazquez, 2000) ages in the Bahía Concepción area, and 91.2 ± 2.1 Ma in the Santa Rosalia area (Schmidt, 1975). Alternatively, the coherent belt of high-amplitude magnetic anomalies present along the Baja California peninsula does not exist in mainland Mexico, suggesting a geological limit located in the Gulf of California (Langenheim and Jachens, 2003).

The crystallization and cooling ages obtained in this study further support this correlation between granitoids of Baja California and the coastal region of Sonora. Batholiths in both areas are the product of continental arc magmatism active during Cretaceous to Tertiary time. This magmatic arc began its activity at around 105 Ma, forming first the eastern Peninsular Ranges batholith (EPRB), and migrating later further to the east where the CSB and younger plutons in central and eastern Sonora were generated (Roldán-Quintana, 1991; Valencia-Moreno *et al*., 2001; Valencia-Moreno *et al.*, 2006). The arc migration has been associated with a change in the subduction angle, which was responsible for the synchronous Laramide orogeny in the region. The eastward migration is underlined by changes in the geochemical characteristics (Damon *et al*., 1983a). The westernmost plutons are slightly more mafic, and consist mainly of low-K granodiorite and tonalite, which are common in the CSB and EPRB, whereas eastern plutons are more alkaline (Valencia-Moreno *et al*., 2003). The similarity in the geochemical characteristics and isotopic ages of the CSB and EPRB, suggest a genetic relationship between them. The ages of crystallization in the EPRB are

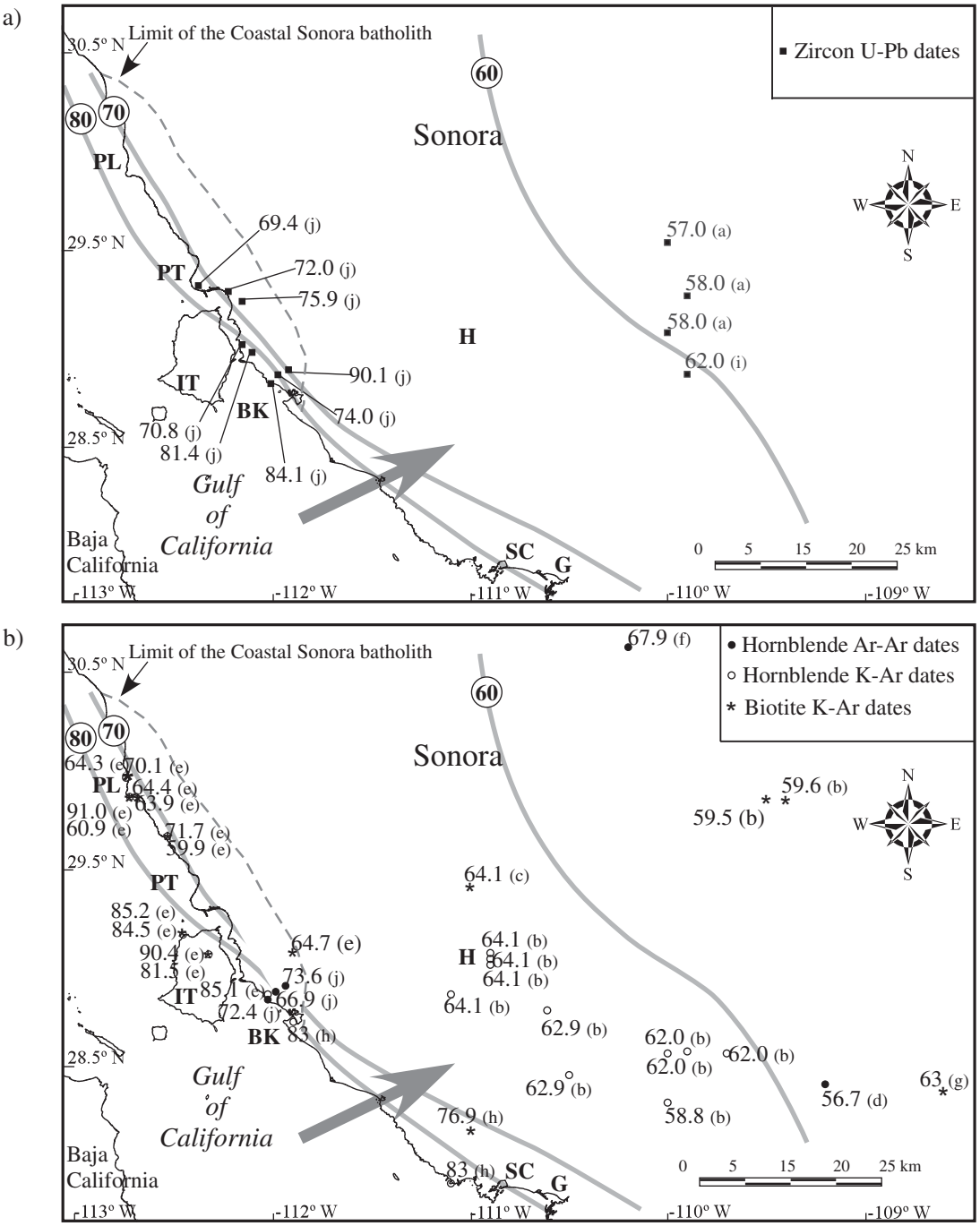

Figure 7. Spatial distribution of isotopic ages for Laramide intrusive rocks in NW Sonora. a: zircon U-Pb dates; b: hornblende and biotite Ar-Ar and K-Ar dates. In both figures, isochrones have been interpreted with the U-Pb data, and the grey arrow shows the direction of migration of the magmatic arc. Sources: (a) Gastil and Krumennacher (1977); (b) Anderson *et al.* (1980); (c) Damon *et al*. (1983a); (d) Damon *et al.* (1983b); (e) Poole *et al*. (1991); (f) Mora-Alvarez (1992); McDowell and Roldán-Quintana (1993); (h) Gans (1997); González-León *et al*. (2000); and (i) this study. BK: Bahía Kino, G: Guaymas, H: Hermosillo, IT: Isla Tiburón, PL: Puerto Libertad, PT: Punta Tepopa, SC: San Carlos.

older than 95 Ma (Ortega-Rivera, 1997; Kimbrough *et al*., 2001), whereas the ages of the CSB are constrained between 90.1 and 69.4 Ma. In central and eastern Sonora, ages vary between ~78 and 57 Ma (Anderson *et al*., 1980; Poole *et al*., 1991). If we restore the peninsula of Baja California to its paleogeographic position before the opening of the Gulf of California (Gastil and Krummenacher, 1977; Oskin, 2002; Ortega-Rivera, 2003), the isotopic age distribution define continuous isochrones from the Baja California peninsula to the interior of Mexico (Damon *et al.*, 1983b; Ortega-Rivera, 2003).

Furthermore, the offset of the contour of the 0.706 ini-

tial $^{87}Sr/^{86}Sr$ isopleth on both sides of the Gulf of California confirms the magnitude of dextral shearing across the Gulf obtained from a comparison between Miocene volcanic rocks from San Felipe area and Bahía Kino areas (Oskin and Scott, 2002).

CONCLUSIONS

The new U-Pb zircon and $^{40}Ar/^{39}Ar$ biotite and K-feldspar geochronology allow us to constrain ages of crystallization and decipher the thermal evolution after emplacement of the successive intrusions of the CSB, and to propose a regional correlation with other plutons of the Laramide magmatic arc. From older to younger magmatic units, the CSB consist of the Puerto Rico diorite, the Kino granodiorite, the Puerto Nuevo granite, and the Tepopa tonalite, as well as the Tordillo andesite as an associated subvolcanic unit. ^{206}Pb-^{238}U zircon ages show that the interval between granodiorite and tonalite crystallization is ~21 Ma (between 90.1 ± 1.1 and 69.4 ± 1.2 Ma), which suggests that during this time interval there was no migration of the magmatic arc along the present coast of Sonora. $^{40}Ar/^{39}Ar$ and K-Ar ages are in agreement with ^{206}Pb -^{238}U zircon ages, and corroborate previous results obtained in that region (Anderson and Silver, 1969; Gastil and Krummenacher, 1977; Mora-Alvarez, 1992; Roldán-Quintana, 2002); they indicate a relatively slow cooling rate of the CSB, between zircon crystallization and closure temperature of K-feldspar. The spatial distribution of ages, older to the south and younger to the north, suggests that the CSB coincide with the transition of the 70–60 Ma isochrons in the model proposed by Ortega-Rivera (2003). The ages determined for the CSB are younger, and consecutive, to those of the EPRB, which is interpreted to belong to the same magmatic arc that migrated eastwards along the continental margin of North America.

ACKNOWLEDGMENTS

This research was supported by the Conacyt research grant 36225 T. We want to thank George Gehrels for access and facilities of Isotope Geochemistry Laboratory of University of Arizona, in Tucson. Also we thank Michael Kunk for access and close supervision of $^{40}Ar/^{39}Ar$ geochronology at the U.S. Geological Survey Thermochronology Laboratory in Denver, Colorado. We also thank Alice Kaminski, a former University of Colorado at Boulder student for careful mineral separations for the Ar/Ar geochronology studies. We thank Pablo Peñaflor-Escárcega for his help in sample preparation at ERNO geochemical laboratory in Hermosillo, Sonora, and René Delgado-González for his field assistance in Baja California. Finally we are grateful to Margarita López Martínez, Luis A. Delgado Argote and Marty Grove for their helpful review of the manuscript.

REFERENCES

Alexander, E.C., Jr., Mickelson, G.M., Lanphere, M.A., 1978, Mmhb-1: a new $^{40}Ar/^{39}Ar$ dating standard, *in* Zartman, R.E. (ed.), Short Papers of the Fourth International Conference, Geochronology, Cosmochronology, and Isotope Geology: U.S. Geological Survey, Open-File Report 78-701, 6-8.

Anderson, T.H., Silver, L.T., 1969, Mesozoic magmatic events of the northern Sonora coastal region, Mexico (abstract): Geological Society of America Abstracts with Programs, 3-4.

Anderson, T.H., Silver, L.T., Salas, G.A., 1980, Distribution and U-Pb isotope ages of some lineated plutons, northwestern Mexico: Geological Society of America, Memoir 153, 269-283.

Barton, M.D., Staude, J.M., Zurcher, L., Megaw, P.K.M., 1995, Porphyry cooper and other intrusion-related mineralization in Mexico, *in* Pierce, E.W., Bolm, J.G. (eds.), Porphyry Cooper Deposits of the American Cordillera: Arizona Geological Society Digest, 99, 674-685.

Busby, C.J., Smith, D.P., Morris, W.R., Adams, B., 1998, Evolutionary model for convergent margins facing large ocean basins: Mesozoic Baja California (Mexico): Geology, 26(3), 227-230.

Cebula, G.T., Kunk, M.J., Mehnert, H.H., Naeser, C.W., Obradovich, J.D., Sutter, J.F., 1986, The Fish Canyon Tuff: A potential standard for the $^{40}Ar/^{39}Ar$ and fission track dating methods: Terra Cognita, 6(2), 140.

Coney, P.J., Reynolds, S.J., 1977, Cordilleran Benioff zones: Nature, 270, 403-406.

Dalrymple, G.B., Alexander, E.C., Lanphere, M.A., Kraker, G.P., 1981, Irradiation of samples for $^{40}Ar/^{39}Ar$ dating using the Geological Survey TRIGA reactor: U.S. Geological Survey, Professional Paper 1176, 55 p.

Damon, P.E., Shafiquillah, M., Clark, K.F., 1983a, Geochronology of the porphyry copper deposits and related mineralization of Mexico: Canadian Journal of Earth Sciences, 20, 1052-1071.

Damon, P.E., Shafiqullah, M., Roldán-Quintana, J. And Cochemé, J.J., 1983b, El batolito Laramide (90-40 Ma) de Sonora: Guadalajara, Asociación de Ingenieros de Minas, Metalurgistas y Geólogos de México (AIMMGM), Memoria técnica XV, 63-95.

Deino, A.L., 2001, Users manual for Mass Spec v. 5.02: Berkeley Geochronology Center, Special Publication 1a, 119 p.

Dickinson, W.R., 1989, Tectonic setting of Arizona through geologic time, *in* Jenney, J.P., Reynolds, S.J. (eds.), Geological Evolution of Arizona: Tucson, Arizona Geological Society Digest, 17, 1-16.

Dickinson, W.R., Gehrels, G.E., 2003, U-Pb ages of detrital zircons from Permian and Jurassic eolian sandstones of the Colorado Plateau, USA: Paleogeographic implications: Sedimentary Geology, 163, 29-66.

Dickinson, W.R., Lawton, T.F., 2001, Carboniferous to Cretaceous assembly and fragmentation of Mexico: Geological Society of America Bulletin, 113, 1142-1160.

Fleck, R.J., Sutter, J.F., Elliot, D.H., 1977, Interpretation of discordant $^{40}Ar/^{39}Ar$ age spectra of Mesozoic tholeiites from Antarctica: Geochimica et Cosmochimica Acta, 41, 15-32.

Gans, P.B., 1997, Large-magnitude Oligo-Miocene extension in southern Sonora: Implications for the tectonic evolution of northwest Mexico: Tectonics, 16, 388-408.

Gastil, R. G., 1975, Plutonic zones in the Peninsular Ranges of southern California and northern Baja California: Geology, 3, 361-363.

Gastil, R.G., 1983, Mesozoic and Cenozoic granitic rocks of southern California and western Mexico, *in* Roddick, J.A. (ed.), Circum-Pacific Plutonic Terranes: Boulder, Colorado, Geological Society of America, Memoir 159, 265-275.

Gastil, G., Krummenacher, D., 1977, Reconnaissance geology of coastal Sonora between Puerto Lobos and Bahia Kino: Geological Society of America Bulletin, 88, 189-198.

Gastil, R.G., Morgan, G.J., Krummenacher, D., 1981, The tectonic history of peninsular California and adjacent Mexico, *in* Ernst, W.G., (ed.), The Geotectonic Development of California: Englewood Cliffs, New Jersey, Prentice-Hall, 284-306.

Gehrels G., Valencia V., Pullen A., 2006, Detrital zircon geochronology by

Laser-Ablation Multicollector ICPMS at the Arizona LaserChron Center, *in* Olszewski, T.D. (ed), Geochronology Emerging Opportunities: Paleontological Society Papers, 12, 67-76.

González-León, C.M., McIntosh, W.C., Lozano-Santacruz, R., Valencia-Moreno, M.A., Amaya-Martínez, R., Rodríguez-Castañeda, J.L., 2000, Cretaceous and Tertiary sedimentary, magmatic, and tectonic evolution of north-central Sonora, NW Mexico: Geological Society of America Bulletin, 112, 600-610.

Gromet, L.P., Silver, L.T., 1987, REE variations across the Peninsular Ranges batholith: Implications for batholith petrogenesis and crustal growth in magmatic arcs: Journal of Petrology, 28, 75-125.

Henry, C.D., McDowell, F.D., Silver, L.T., 2003, Geology and geochronology of the granitic batholithic complex, Sinaloa, México: Implications for Cordilleran magmatism and tectonics, *in* Johnson, S.E., Paterson, S.R., Fletcher, J.M., Girty, G.H., Kimbrough, D.L., Martin-Barajas, A. (eds.), Tectonic evolution of western Mexico and the Southwestern USA: Boulder, Colorado, Geological Society of America, Special Paper 374, 237-274.

Iriondo, A., Kunk, M.J., Winick, J.A., Consejo de Recursos Minerales, 2003, $^{40}Ar/^{39}Ar$ dating studies of minerals and rocks in various areas in Mexico; USGS/CRM Scientific Collaboration (Part I): U.S. Geological Survey Open File Report, OF-03-020, 79 p.

Iriondo, A., Kunk, M.J., Winick, J.A., Consejo de Recursos Minerales, 2004, $^{40}Ar/^{39}Ar$ dating studies of minerals and rocks in various areas in Mexico; USGS/CRM Scientific Collaboration (Part II): U.S. Geological Survey Open File Report, OF-04-1444, 46 p.

Johnson, S.E., Tate, M.C., Fanning, C.M., 1999, New geologic mapping and SHRIMP U-Pb zircon data in the Peninsular Ranges Batholith, Baja California, Mexico: Evidence for a suture?: Geology, 27, 643-746.

Kimbrough, D.L., Smith, D.P., Mahoney, J.B., Moore, T.E., Grove, M., Gastil, R.G., Ortega-Rivera, A., Fanning, C.M., 2001, Forearc-basin sedimentary response to a rapid late Cretaceous batholith emplacement in the Peninsular ranges of southern and Baja California: Geology, 29, 491-493.

Kistler, B.W., Wooden, J.L., Morton, D.M., 2003, Isotopes and ages in the northern Peninsular ranges batholith, southern California: U.S. Geological Survey, Open File Report 2003-489, 45 p.

Kunk, M.J., Sutter, J.F., Naeser, C.W., 1985, High-precision $^{40}Ar/^{39}Ar$ ages of sanidine, biotite, hornblende, and plagioclase from the Fish Canyon Tuff, San Juan Volcanic Field, south-central Colorado: Geological Society of America Abstracts with Programs, 17, 636.

Langenheim, V.E., Jachens, R.C., 2003, Crustal structure of the Peninsular Ranges batholith from magnetic data: Implications for Gulf of California rifting: Geophysical Research Letters, 30(11), 1597, doi:10.1029/2003GL017159.

Ledesma-Vázquez, J., 2000, Cuencas sedimentarias del Plioceno en el Golfo de California; Cuenca San Nicolás, B.C.S.: Ensenada, México, Facultad de Ciencias Marinas, Ph. D. Thesis, 171 p.

Ludwig, K.R., 2003, User's manual for Isoplot 3.00: A geochronological toolkit for Microsoft Excel, Berkeley Geochronology Center, Special Publication 4, 1-70.

McDougall, I., Harrison, T.M., 1999, Geochronology and Thermochronology by the $^{40}Ar/^{39}Ar$ Method: Oxford University Press, 269 pp.

McDowell, F.W., Mauger, R.L., 1994, K-Ar and U-Pb zircon geochronology of Late Cretaceous and Tertiary magmatism in central Chihuahua State, Mexico: Geological Society of America Bulletin, 106, 118-132.

McDowell, F.W., Roldán-Quintana, J., 1993, Geochronology of Mesozoic-Cenozoic magmatism in south-central Sonora: A progress report, *in* González-León, C., Vega-Granillo, L. (eds.), III Simposio de la Geología de Sonora y áreas adyacentes, libro de resúmenes: Hermosillo, Sonora, Instituto de Geología (UNAM) and Departamento de Geología (UNISON), 77-80.

McDowell, F.W., Roldán-Quintana, J., Connelly, J.N., 2001, Duration of Late Cretaceous–early Tertiary magmatism in central Sonora, Mexico: Geological Society of America Bulletin, 113, 521-531.

McFall, C.C., 1968, Reconnaissance geology of the Concepción Bay area, Baja California, Mexico: Stanford University, Publications of Geological Sciences, 10 (2).

Mora-Alvarez, G., 1992, History of the Cenozoic magmatism in the Sierra Santa Ursula, Sonora, Mexico: Austin, TX, University of Austin, M.S. Thesis, 153 p.

Mora-Alvarez, G., McDowell, F.W., 2000, Miocene volcanism during late subduction and early rifting in the Sierra Santa Ursula of western Sonora, Mexico, *in* Delgado-Granados, H., Aguirre-Díaz, G., Stock J.M. (eds.), Cenozoic Tectonics and Volcanism of Mexico: Geological Society of America, Special Paper 334, 123-141.

Ortega-Rivera, A., 1997, Geochronological constraints on the thermal and tilting history of the Peninsular Ranges batholith of Alta California and Baja California: Tectonic implications for southwestern North America (Mexico): Kingston, Ontario, Canada, Queen's University, Department of Geological Sciences, Ph.D. Thesis, 582 p.

Ortega-Rivera, A., 2003, Geochronological constraints on the tectonic history of the Peninsular Ranges batholith of Alta and Baja California: Tectonic implications for western Mexico, *in* Johnson, S.E., Paterson, S.R., Fletcher, J.M., Girty, G.H., Kimbrough, D.L., Martin Barajas, A. (eds.), Tectonic Evolution of Western Mexico and the Southwestern USA: Boulder, Colorado, Geological Society of America, Special Paper 374, 297-335.

Oskin, M., 2002, Tectonic evolution of the northern Gulf of California, Mexico, deduced from conjugate rifted margind of the Upper Delfín Basin (Part I): Pasadena, California, California Institute of Technology, Ph.D. Thesis, 481 p.

Oskin, M., Scott, J., 2003, Pacific-Northe America plate motion and opening of the Upper Delfín basin, northern Gulf of California, Mexico: Geological Society of America Bulletin, 115, 1173-1190.

Poole, F.G., Madrid, R.J., Oliva-Becerril, F., 1991, Geological setting and origin of the stratiform barite in central Sonora, Mexico, *in* Raines, G.L., Lisle, R.E., Scafer, R.W., Wilkinson, W.H. (eds.), Geology and Ore Deposits of the Great Basin: Reno, Nevada, Geological Society of Nevada, 1, 517-522.

Pupin, J. P., 1983, Zircon and granite petrology: Contributions to Mineral Petrology, 73, 207-220.

Roldán-Quintana, J., 1991, Geology and chemical composition of the Jaralito and Aconchi batholiths in east-central Sonora, México, *in* Pérez-Segura, E., Jaques-Ayala, C. (eds.), Studies of Sonoran Geology: Boulder, Colorado, Geological Society of America, Special Paper 254, 69-80.

Roldán-Quintana, J., 2002, Caracterización geológico-geoquímica y evolución del arco magmático mesozoico-terciario entre San Carlos y Maycoba, sur de Sonora: México, D.F., Universidad Nacional Autónoma de México, Instituto de Geología, Ph.D. Thesis, 185 p.

Schaaf, P., Bohnel, H., Pérez-Venzor, J.A., 2000, Pre-Miocene palaeogeography of the Los Cabos Block, Baja California Sur: geochronological and palaeomagnetic constraints: Tectonophysics, 318, 53-69.

Shafiqullah, M., Damon, P., Clark, K.E., 1983, K-Ar chronology of Mesozoic-Cenozoic continental magmatic arcs and related mineralization in Chihuahua, *in* Clark, K.F., Goodel, P.C. (eds.), Geology and Mineral Resources of North-Central Chihuahua: El Paso, Texas, El Paso Geological Society, Guidebook, 303-315.

Schmidt, E.K., 1975, Plate tectonics, volcanic petrology, and ore formation in the Santa Rosalía area, Baja California, Mexico, *in* Frizell, V.F. (ed.), Society of Economic Paleontologists and Mineralogists, Special Publication, 237-251.

Silver, LT., Chapell, B., 1988, The Peninsular Ranges batholith: An insight into the Cordilleran batholiths of southwestern North America: Transactions of Royal Society of Edimburgh, Earth Sciences, 79, 105-121.

Silver, L.T., Taylor, H.P., Chapell, B., 1979, Some petrological, geochemical, and geochronological observations of the Peninsular Ranges batholith near the international border of the U.S.A. and Mexico, *in* Abott, P.L., Todd, V.R., (eds.), Mesozoic Crystalline Rocks: Geological Society of America, Annual Meeting, Guidebook, 83-110.

Snee, L.W., Sutter, J.F., Kelly, W.C., 1988, Thermochronology of economic mineral deposits: Dating the stages of mineralization at Panasqueira, Portugal, by high precision $^{40}Ar/^{39}Ar$ age spectrum techniques on muscovite: Economic Geology, 83, 335-354.

Stacey, J.S., Kramers, J.D., 1975, Approximation of terrestrial lead isotope evolution by two-stage model: Earth and Planetary Sciences Letters, 26, 207-221.

Staude, J.M.G., Barton, M.D., 2001, Jurassic to Holocene tectonics, magmatism, and metallogeny of northwestern Mexico: Geological Society of America Bulletin, 113 (10), 1357-1374.

Steiger, R.H., Jäger, E., 1977, Subcommission on geochronology: Convention on the use of decay constants in geo- and cosmochronology: Earth and Planetary Science Letters, 36, 359-363.

Stock, J.M., Hodges, K.V., 1989, Pre-Pliocene extension around the Gulf of California and the transfer of Baja California to the Pacific plate: Tectonics, 8 (1), 99-115.

Thomson, C.N., Girty, G.H., 1994, Early Cretaceous intro-arc ductile strain in Triassic-Jurassic and Cretaceous continental margin arc rocks, Peninsular Ranges, California: Tectonics, 13, 1108-1119.

Valencia-Moreno, M.A., 1998, Geochemistry of Laramide granitoids and associated porphyry copper mineralization in NW Mexico: Tucson, Arizona, University of Arizona, Ph.D. Thesis.

Valencia-Moreno, M., Ruiz, J., Roldán-Quintana, J., 1999, Geochemistry of Laramide granitic rocks across the southern margin of the Paleozoic North American Continent, central Sonora, México: International Geology Review, 41, 845-857.

Valencia-Moreno, M., Ruiz, J., Barton, M.D., Patchett, P.J., Zurcher, L., Hodkinson, D.G., Roldán-Quintana, J., 2001, A chemical and isotopic study of the Laramidic granitic belt of northwestern México: Identification of the southern edge of the North American Precambrian basement: Geological Society of America Bulletin, 113(11), 1409-1422.

Valencia-Moreno, M., Ruiz, J., Ochoa-Landín, L., Martínez-Serrano, R., Vargas-Navarro, P., 2003, Geochemistry of the Coastal Sonora Batholith, Northwestern México: Canadian Journal of Earth Sciences, 40(6), 819-831.

Valencia-Moreno, M., Iriondo, A., González-León, C., 2006, Temporal constraints on the eastward migration of the Late Cretaceous-Early Tertiary magmatic arc of NW Mexico based on new $^{40}Ar/^{39}Ar$ hornblende geochronology of granitic rocks: Journal of South American Earth Sciences, 22(1-2), 22-38.

Vargas-Navarro, P.P., 2002, Geología y geoquímica del Batolito Costero de Sonora entre Bahía Kino y Punta Chueca: Hermosillo, Sonora, Universidad de Sonora, Departamento de Geología, B.S. Thesis, 83 p.

Vernon, R.H., 2000, Review of microstructural evidence of magmatic solid-state flow: Electronic Geosciences, 5(2), 23 p.

Vidal-Solano, J.,R., Paz-Moreno, F.A., Iriondo, A., Demant, A., Cochemé, J.J., 2005, Middle Miocene peralkaline ignimbrites in the Hermosillo region (Sonora, México). Geodynamic implications: Comptes-Rendus Geoscience, 337, 1421-1430.

Walawender, M.J., Gastil, R.G., Clinkenbeard, J.P., McCormick, W.V., Eastman, B.G., Wardlaw, R.S., Gunn, S.H., Smith B.M., 1990, Origin and evolution of the zoned La Posta–type plutons, eastern peninsular Ranges Batholith, southern and Baja California, *in* Anderson, J.L. (ed.), The Nature and Origin of Cordilleran Magmatism: Geological Society of America, Memoir 174, 1-18.

Walawender, M.J., Girty, G.H., Lombardi, M.R., Kimbrough, D., Girty, M.S., Anderson, C., 1991, A synthesis of recent work in the Peninsular Ranges batholith, *in* Walawender, M.J., Hanan, B.B., (eds.), Geological Excursions in Southern California and Mexico: San Diego, U.S.A., San Diego State University, Department of Geological Sciences, 297-312.

Wetmore, P.H., 2003, Investigation into the tectonic significance of the along strike variations of the Peninsular Ranges Batholith, southern and Baja California: Los Angeles, U.S.A., University of Southern California, Ph.D. Thesis, 186 p.

Wetmore, P.H., Schmidt, K.L., Paterson, S.R., Herzig, C., 2002, Tectonic implications for the along-strike variations of the Peninsular Ranges batholith, southern and Baja California: Geology, 30, 247-250.

Wodziki, W.A., 1995, The evolution of Laramide igneous rocks and porphyry copper mineralization in the Cananea district, Sonora, Mexico: Tucson, Arizona, University of Arizona, Ph.D. Thesis, 183 p.

Manuscript received: April 10, 2007
Corrected manuscript received: February 26, 2008
Manuscript accepted: March 11, 2008